Summer 2025

The Role of Symmetries in Atomic, Electromagnetic, and Particle Physics

Joshua Martin O'Connor
University of South Carolina

The Role of Symmetries in Atomic, Electromagnetic, and Particle Physics

by

Joshua Martin O'Connor

Bachelor of Science
University of South Carolina 2020

Submitted in Partial Fulfillment of the Requirements

for the Degree of Doctor of Philosophy in

Physics

College of Arts and Sciences

University of South Carolina

2025

Accepted by:

Brett Altschul, Major Professor

Matthias Schindler, Committee Member

Alexey Petrov, Committee Member

Ralf Lehnert, Committee Member

Anne Vail, Dean of the Graduate School

Dedication

To my loving wife, Jodi Michele with all my heart and gratitude. And to our beautiful creations: Owen Tate, Talan Cole and Sadie Claire.

Acknowledgments

I first thank my professors for letting me tag along and learn (or most of the time at least, attempt to learn) how to become a professional scientist. I would have used the words "leading scientist," but this would be an overstatement because the training I received from them showed me how much respect they deserve for they are top tier physicists and world leading experts who were trained by some of the best physicists in history: such as my advisor's advisor; Roman Jackiw or his advisor; Hans Bethe.

I give my deepest and most intimate gratitude to both Brett Altschul and Matthias Schindler for working with me and for their time spent in very useful discussions and insights—to Brett Altschul for introducing me to the great John David Jackson in my first year of graduate school and for being my advisor over the past couple of years. I further thank Brett Altschul for his very useful advice, extremely interesting ideas, developments which lead to increasing my knowledge and productivity and for leading me towards the path to success. Thank you very much as well to Matthias Schindler for introducing me to advanced quantum theory, advising me in my final semester, and for opening the door to other advanced and extremely interesting possible directions which could be taken to further what has already been developed. The author also would like to thank with his best gratitude Ralf Lehnert and Alexey Petrov for willing to be committee members for his dissertation; also to Ralf Lehnert for invitations to his CPT meetings (where so much knowledge was gained) and for

collaborations with him and members affiliated with his college and the SME group; and to Alexey Petrov for next level insights, great discussions and allowing me to do research and teach in the Department of Physics and Astronomy during my time at the University of South Carolina. Finally, extreme thanks and more gratitude also go to Varsha Kulkarni for showing me how to teach and for the opportunity to work with high-caliber students. Thank you very much also to Varsha Kulkarni for providing the teaching assistant job that helped to provide for my family during the years while I was in school and heavily involved in research.

Abstract

Symmetries in atomic, electromagnetic, and weak interaction physics are explored to understand symmetry-breaking extensions of the Standard Model of particle physics. Lorentz-violating field theories are extremely interesting theoretically, since they possess many new features that are absent in Lorentz-invariant models. We outline the formalism and experimental status of the Lorentz- and CPT-violating Standard Model Extension, in both the classical and quantum regimes. Processes such as vacuum Cerenkov radiation, which are kinematically forbidden when Lorentz symmetry is exact may become allowed when this symmetry is weakly broken. Particle decays, such as pion and kaon decays, although allowed in Lorentz-invariant theories, are also used as tools to probe Lorentz violation. For example, in pion decay, it is possible to have Lorentz violation in both the W-boson and muon sectors. We look at two separate sectors of the extended theory, with preferred axial-vector and tensor backgrounds, respectively.

Following introductory remarks, the general framework for models of extending Standard Model physics to account for possible Lorentz violation is laid out. Experimental bounds are given for the Lorentz-violating parameters used in our work, along with a few others for comparisons to other types of models that could be worked on in similar future analyses. In our first model, we analyze a modification to electromagnetism involving vacuum-birefringence effects in the photon sector, by searching

for symmetry-breaking in the classical Larmor radiation formula. For the second analysis, we analyze a three-particle decay process with Lorentz symmetry broken in each of the three outgoing particle's energy-momentum relation. We obtain new decays rates and Dalitz plot outlines. The analysis of possible extensions of this type of work in future research is discussed, including how precision measurements could be of use in constraining the Lorentz violation coefficients for spinless three-particle decay processes.

Table of Contents

List of Tables

List of Figures

Chapter 1

Introduction

Considerations of symmetries in physics are part of the basis of every theory. One of the most interesting questions one could ask for motivation is: What might be the fundamental symmetries of the underlying description of nature? To get the correct solution to this question one must first know what is meant by fundamental symmetry and how nature is described. The validity of physical theories are often tested using symmetry transformations, which involve changing the physical or observational point of view but still yield the same experimental results if the symmetry holds. The main symmetries needed to explain particle interactions may be continuous or discrete, and they may also be exact or only approximate. Specific important symmetries include Lorentz and gauge symmetries, which are particularly key to our understanding of nature.

James Clerk Maxwell, Hendrick Lorentz, Henri Poincaré, Albert Einstein, and Paul Dirac were some of the most important founding fathers of modern physics. They gave us insights into the way the world is by making discoveries of new physical laws and developing theories that could be tested; this program ultimately developed into the modern study of Lorentz symmetry. The first noteworthy experimental tests to try to find inconsistencies with these newly developed physical laws were carried out in 1887 by Michelson and Morely, well before understanding Lorentz symmetry was complete. The special theory of relativity (describing the meaning of Lorentz transformations) underlies all of fundamental physics as we currently understand it—including the general theory, as well as relativistic quantum field theory. For standard relativistic theories, invariance under local Lorentz transformations is a requirement. The associated Lorentz symmetry ensures that all physical laws obey

Einstein's principle of relativity, which states the equivalence of certain "inertial" frames of reference; the laws of physics are identical for all observers that move at constant velocities with respect to one-another. As Maxwell's equations predicted a finite light speed in 1861 and 1862, relativity dictates that this speed of light must be the same for observers in different inertial reference frames. This relativity principle is the basis for Einstein's special and General Relativity (GR). Special relativity and quantum mechanics, in turn, form the bases of the Standard Model (SM) of particle physics. Lorentz symmetry is therefore one of the most important and fundamental properties of the physical world.

Before going into what happens when symmetries in physical theories are broken, we briefly describe standard physics in classical field theory, quantum mechanics, and quantum-field-theoretic particle physics. In classical radiation theory, the concept of a field was originally introduced to account for the interactions between two bodies separated by a finite distance. The classical fields were scalar and three-vector functions defined at each spacetime point. Quantum mechanics is analogous to probability theory. In quantum theory, the field concept acquires a new dimension, and physics is described through a propagating wave function. The current state of the system is uniquely determined by this wave function, in the sense that it allows the computation of all observable quantities. The state function is a vector with complex values in Hilbert space. Given the state of the system at any instant of time (initial state), the Hamiltonian suffices to completely govern its evolution to some later time (final state). Consider a state function at time $t = 0$; then the time evolution is defined by a complex-valued transition amplitude which determines the state func-

tion at a later time t. Complex values result at every stage until the end, when the absolute value of the final state function squared is interpreted as a probability density, from which experimental predictions are made. The further notion of quantum field theory, as developed from the late 1920s to the 1940s, is to associate particles with fields such as the electromagnetic field or the electron field. The wave function from quantum mechanics is taken over into the framework of quantum field theory by taking it to be a multicomponent field that transforms under rotations and boosts according to the Poincaré group. For particles of spin $\frac{1}{2}$, this field is a Dirac spinor. The fields for particles of vanishing spin in the quantum field theory are solutions to the Klein-Gordon equation.

Quantum field theory is essentially quantum mechanics, as applied to dynamical systems made up of continuous fields rather than point particles. Particles that move with relativistic energies are quantized differently from particles in the non-relativistic case. A single particle relativistic equation, either the Klein-Gordon or Dirac equation, gives rise to negative energy states and other inconsistencies. A major tool that physicists use is analysis of energy and momentum, which are conserved by the invariance of the laws of physics under spacetime translations. The symmetries of flat four-dimensional spacetime, otherwise known as Minkowski spacetime, are represented by the Poincaré group, which includes both Lorentz symmetry and these spacetime translations. Einstein's famous $E = mc^2$ allows for the creation of particle-antiparticle pairs, preventing us from being able to assume that we can define any relativistic process in terms of a single particle. There is also the issue of causality—that propagation amplitudes outside the light cone ($\vec{x}^2 > t^2$) may be

nonzero. This is also solved in quantum field theory by realizing that the propagation of a particle across a spacelike interval is indistinguishable from the propagation of an antiparticle in the opposite direction. The amplitudes for the propagation of the particles and antiparticles exactly cancel, and therefore the causality is preserved. Further, define a quantum field theory as "in cone" as one with momenta that are conjugate to the successive spacetime difference variables which are physical or on the forward light cone in momentum space. Similarly, "out of cone" means that unphysical momenta that can be outside the forward light cone are present in addition (possibly) to physical momenta. The quantum field theory thus provides a solution to causality by introducing antiparticles. Most importantly, it provides tools for calculating scattering cross sections, particle lifetimes, and other observable quantities. The extreme accuracy of experiments, which confirm the predictions made by quantum field theory, is the main reason for studying this theory and its possible extensions.

Relativistic quantum field theory represents a marriage of the physics of the tiny (meaning quantum mechanics) and the very fast (special relativity). However, there is a fundamental problem in physical analyses, lying in that gravity (including the physics of very large physical scales) is not included. It is thought that ultimately GR, the geometrical theory of gravitation, and the quantum-mechanical theory of elementary particles should be described through a unified formalism, although so far these theories have proven difficult or impossible to reconcile. The Standard Model explains accurately a variety of physical interactions, although it leaves some important observations unexplained, such as the large dominance of matter over

antimatter in the universe. The Standard Model only gives a description of a tiny piece of the vast and ever-expanding universe and leaves dark matter, dark energy, and quantum gravity unexplained. However, a promising point is that they do in fact share nearly the same local symmetry structures. Both rely on the fact that the laws of physics in each inertial frame are to be invariant under $SO(3,1)$, the Lorentz transformations of $(3+1)$-dimensional spacetime, including rotations and boosts; and the discrete transformations of parity (P) and time reversal (T) and the non-spacetime operation of charge conjugations (C). One origin of the difference in the major theories is that in general relativity, $SO(3,1)$ is a local symmetry of the tangent space at each point of the space-time manifold [9], thus leaving room for exploration. Also, in standard physics, relativistic field theory is invariant under the proper, orthochronous Lorentz group but not P, T, or C individually, only the combination of all three, CPT. However, experiment has verified that three of the four forces of nature: strong (nuclear), electromagnetic, and gravitational, are separately symmetric with respect to C, P, and T.

Moreover, in spite of the problems with gravitation, the quantum field theory framework is accepted as the kind of theory that gives the best description of elementary particles and their interactions. The interactions of quarks and leptons are described by these fields. There are two types of fields, Fermi and Bose fields. Fermi fields describe identical particles that cannot occupy the same state, by the Pauli Exclusion Principle, while a Bose field describes identical particles that can be in the same state. Following Fermi-Dirac statistics are the electrons, protons, and quarks; these fermions must have half-integer spin. Bosons are particles like

photons and π-mesons (or pions), having integer spin and following Bose-Einstein statistics. Quantum field theory fully explains this relationship between spin and particle statistics. A classical Fermi field is a non-commutative analog of a function and is by definition an element of an antisymmetric tensor algebra, called a Grassmann algebra. The generators of the algebra do not commute. The Bose field generators, however, do commute. The Bose fields can be both scalar, vector (including gauge), and tensor fields. An alternative interpretation of gauge fields is that they do not describe quantities associated with individual points, but rather convey how to transport these quantities along curves; for example, the magnetic vector potential can be interpreted as describing how to transport a quantum-mechanical phase along a curve through space.

In a given theory, the discrete symmetries are checked by considering each of C, P, and T as an operator that operates on wave functions and fields, changing various parameters. Parity sends the spatial coordinates ($\vec{x}$) to point in the opposite direction, $\vec{x} \to -\vec{x}$. If a wave function is spatially symmetric or antisymmetric, the corresponding state will have even or odd parity, respectively. For time reversal, which sends $t \to -t$, particle momentum and spin should also be inverted. The third discrete symmetry is the particle-antiparticle symmetry of charge conjugation, which converts a particle with a given spin orientation into an antiparticle with the same spin orientation. All combinations $\bar{\Phi} G \Phi$ (known as Dirac bilinears) of a quantum field (the Dirac spinor Φ), its conjugate, and a constant 4×4 matrix G may be, if G written in terms of the sixteen antisymmetrized products of γ-matrices, decomposed into terms that have definite transformation properties under the Lorentz group.

The five combinations of different types of bilinears (when G is written in terms of tensorial combinations of γ-matrices), when their Lorentz indices are contracted with other vector and tensor objects are therefore invariant under the combined symmetry CPT. This is an indication that CPT is closely connected with Lorentz symmetry. In fact, CPT can only be broken if Lorentz symmetry is also broken, although Lorentz violation does not necessarily imply CPT violation [42].

There are well-developed methodologies for considering physical theories in and beyond the Standard Model of particle physics. Symmetries in the Standard Model of particle physics theory are realized in four main fashions. The simplest case is when a global symmetry is manifest, leading to particle multiplets with restricted interactions. The second is when a global symmetry is spontaneously broken, such as the electroweak gauge symmetry or the Lorentz symmetry. This occurs when the vacuum state is non-invariant but the equations of motion and Lagrangian are invariant, and the particles do not form obvious symmetry multiplets. Instead, in such a theory, spinless particles of zero mass, Goldstone Bosons, will appear (one for each generator of the spontaneously broken symmetry) [47]. When this is generalized to Lorentz symmetry being spontaneously broken, there will be observable tensor backgrounds proportional to the vacuum expectation values of the tensor-valued fields responsible for the symmetry breaking. Thus, tensor backgrounds are of great use in detecting fundamental symmetry violations. As we will explore in depth in the following chapters, the Standard Model is used as a starting point because it explains how elementary particles interact and can be extended to include background fields and tensors [9]. The third way symmetries may be realized in Standard Model physics

is that of a local, or gauge, symmetry; here, symmetry requires the existence of a massless vector field for each symmetry generator, and the interactions among these fields are highly restricted. The fourth symmetry structure considered in standard quantum field theory is if we consider both local gauge invariance and spontaneous symmetry breaking in the same theory. This type requires gauge vector bosons to acquire mass through the well-known Higgs mechanism.

This dissertation outlines methods which could further our understanding of nature and eventually contribute to a correct combination of the Standard Model and General Relativity, which would be one of the greatest discoveries in modern science. The main recipe for the search for discrepancies and symmetry modifications is given, along with up-to-date experimental bounds for the type of specific violations considered in our models. Further analysis, calculations, conclusions, and results for my research are included in chapters 3 and 4. Specifically, in this dissertation work two major physical situations are resolved. In the first case, we consider the radiation from a harmonically oscillating electric dipole in a modified theory of electromagnetism, seeking to see how the character of classical radiation would change in the presence of a preferred spacetime direction. The second focuses on tensorial Lorentz violation, and how momentum and energy are modified and what implications this has on the dynamics and kinematics of specific particle processes. The results and extensions of this research work are discussed and described. In closing, there is an overall summary of my research and possible extensions to our models, plus considerations of future possible routes that could be interesting and further our understanding of nature.

Chapter 2

Broken Symmetry in the Standard Model Extension

2.1 Theoretical Framework

In the Standard Model, physics must be identical in each inertial frame: invariant under Lorentz transformations. However, we relax this notion and implement particle theory models in inertial frames where the physics is modified. These Lorentz non-invariant theories contain inertial frames that are not all equivalent. This makes necessary changes to specific calculation procedures used in the standard model; we can obtain completely or slightly modified observable values or predict new physical phenomena that can also be measured. For example, changes in the standard energy-momentum relations for various types of quanta can affect the rates and thresholds for particle processes. In this section, we consider the implications of Lorentz non-invariance and how it may be applied to various models. The experimental bounds for these types of processes are included in the next section [105].

Theories with Lorentz symmetry-breaking frames are of interest, since quantum theories of gravitation may not have the same symmetries as the low-energy effective theories that we see in everyday operation. Theories of Planck-scale physics such as string theory, loop quantum gravity, non-commutative spacetime structures, space-time foam, non-trivial spacetime topologies, and others already predict or strongly suggest Lorentz violation [107, 106, 81, 58, 44, 40, 59, 92, 45, 39, 67, 87, 43, 52]. The same tools used to study the Standard Model may also be used to analyze more general theories in which the Lorentz symmetry is weakly broken.

There have always been questions—both theoretical and empirical—about whether special relativity as it was introduced by Einstein in 1905 truly represents an exact local symmetry structure for spacetime or whether it is merely an extremely accu-

rate approximate model. In the twentieth century and beyond, the study of apparent symmetries that are eventually discovered to be not exactly but only approximately valid has become extremely important and has provided many fruitful insights about the fundamental interactions of nature. However, experimental tests of relativity and theoretical analyses of test theories with broken Lorentz symmetry were not really approached in a systematic fashion until the 1990s. Using modern Effective Field Theory (EFT), it became comparatively straightforward to parameterize very general test theories for Lorentz violation in particle physics and gravitation. It turns out that these systematic EFTs allow for much wider arrays of types of anisotropy and Lorentz-boost violation than had previously been examined. These theoretical developments were followed by an upsurge in experimental interest in Lorentz-symmetry tests because it was realized that there was a much broader landscape of potentially symmetry-violating phenomena. So far, new generations of experiments have not found any convincing evidence of Lorentz violation, but increasingly precise tests have continued to be a significant area of research. One key reason for the continued interest is that, however unlikely Lorentz violation is deemed to be, if it is ever confirmed experimentally, that it would be such a profound discovery that it would change a lot what we think we understand about the fundamental nature of the universe we live in.

It is now well understood how to set up the general local EFT that describes Lorentz-violating modifications to the physics of known Standard Model species [33, 34]. This EFT, known as the Standard Model Extension (SME), is also capable of describing all stable, unitary, and local forms of CPT violation, because of the

close connections between CPT violation and Lorentz violation in theories with well-defined S-matrices [42]. Moreover, the SME can also be expanded to cover gravitation [60], although the extension to metric theories of gravity creates additional complications beyond those seen in the particle physics sector [83, 35, 86]. Part of the reason for this is that the particle sector of the SME is formulated using the language of quantum field theory (QFT), just like the Standard Model, while metric theories of gravity (like general relativity and its generalizations) are not really understood beyond the classical level. The main complications when introducing gravity and quantum mechanics in our SME is thus that a local, stable, unitary, CPT-violating quantum field theory is also necessarily Lorentz violating [42].

As the SME is an effective field theory, it contains towers of operators of increasing mass dimension, with the contributions from higher-dimensional operators assumed to be further suppressed under most circumstances. The minimal SME is a restricted subtheory of the SME—that which is expected to be renormalizable, because it satisfies the usual conditions that ensure renormalizability for the Standard Model, by containing only the finite number of local, Hermitian, gauge-invariant operators which can be built out of the known Standard Model fermion and boson field that are of dimension four or less. The terms in the minimal SME Lagrange density are, in structure, very similar to those appearing the usual Standard Model; the key difference is that the additional Lorentz-violating operators each have one or more uncontracted Lorentz indices. The coefficients multiplying those operators then become observable as components of preferred background vectors or tensors. In many situations, the minimal SME is the most natural test theory for analyzing

the results of experimental searches for CPT or Lorentz violation. In general, the SME may be thought of as a structure that enables scientists to translate the absence of experimentally observed signs of Lorentz violation into constraints on other meaningful physical quantities to be measured [68].

Here we shall be considering a Lorentz non-invariant theory along these lines. Many elementary aspects of the general SME remain somewhat mysterious and are open opportunities for prospective research. Field theories with atypical properties can, even if those field theories are never likely to be physically realized, provide useful theoretical laboratories for understanding how quantum theories in general can behave; pure massless quantum electrodynamics in $1+1$ dimensions is unlikely to exist physically, but that did not prevent the Schwinger model [94, 26] from educating us about the fact that there may sometimes be an infinite number of vacua with different topologies. Gauge invariance properties and radiative corrections to the SME effective field theory have, as a result, achieved a plethora of theoretical attentions [88, 84, 29, 75, 98, 10, 11].

So we search for Lorentz violating effects but still implement most of the tools used in Standard Model physics. We add putative Lorentz-violating backgrounds but do so in a way where the theory is still local, keeps gauge invariance intact, and follows standard relativistic quantum mechanics conventions. A quantum field theory is Lorentz covariant "in cone" if vacuum matrix elements of unordered products of field, the Wightman functions, are covariant. The SME also assumes in-cone Lorentz covariance, equivalent to Poincaré covariance. The underlying vacuum matrix elements are calculated in terms of time ordered products of fields (τ functions) which

must be covariant to ensure the quantum field theory is covariant as well. The τ or similar functions like the retarded or advanced products (R or A functions) are used to calculate scattering matrices. To have a Lorentz invariant theory, it is required to have both in- and out-of-cone covariance; both the Wightman and τ (or R or A) functions must be covariant for the theory to be Lorentz covariant. Moreover, weak local commutativity at spacetime points in which all convex combinations of the successive differences are spacelike, is a necessary condition for the CPT symmetry.

In beyond Standard Model physics, we typically add novel backgrounds to weakly break symmetry in a way where the theory is still local. However, locality in the quantum field theory can have three different meanings. One is that the fields must enter terms in the Hamiltonian and the Lagrangian at the same spacetime point. Two, the observables commute at spacelike separations. Three, integer spin fields, representing bosons, commute, and fields for fermions, with half-integer spins, must anticommute, both at spacelike separations. Already in the Standard Model there are cases where one or more of the conditions do not hold. For example, the first requirement fails in quantum electrodynamics in the Coulomb gauge. A further example is in parastatistics theories of order greater than one, where third point fails [42].

Our calculationally consistent theory uses a Lagrangian that is further highly restricted by conditions of renormalizability and gauge invariance. The Standard Model is a theory consisting of a renormalizable Lagrangian that is $SU(3)_c \times SU(2)_L \times U(1)_Y$ symmetric. The forces are mediated by exchange particles; for the strong force this particle is known as the gluon; the weak force is mediated by the W and

Z bosons; and for electrodynamics it is the photon. The strong force is described by the symmetry group of $SU(3)_c$ matrices, where the subscript represents the degree of freedom of colour. The weak force and the electromagnetic, unified in the electroweak interaction, are described in terms of isospin and weak hypercharge quantum numbers. (Although gravity is not included in the Standard Model, that force is mediated by a graviton.) These ideas of local internal symmetries and gauge transformations were introduced long ago. The lack of a renormalizable field theory of massive spin-1 particles raised interest in developing schemes for general non-Abelian gauge theories. Spin-0 and spin-$\frac{1}{2}$ particles are described by the standard methods of field quantization employing the Klein-Gordon and Dirac Lagrangians, respectively.

The minimal SME, which includes Lorentz-violating field operators of mass dimension two, three, and four, will be the domain for our present analysis. Current physical experiments at relatively low energies are useful for testing precisely this low-energy limit of the full SME. Since many low-energy experiments may be extremely precise, they may be more likely than data collected closer to the Planck scale to provide empirical proof of a violation of the symmetries of the current Standard Model. When dealing with electromagnetic phenomena, it is typical to truncate the minimal SME even further to just a minimal Lorentz- and CPT-violating extension of quantum electrodynamics (QED). Although the minimal SME and the minimal QED extension are quantum theories, they exhibit many potentially novel phenomena already at the classical level. In particular, radiation emission may be heavily modified by the presence of the symmetry-breaking terms in the action. For example, in theories in which the maximum speeds of all species are not equal, it is easy to

envision that there could be Cerenkov radiation in vacuum. Careful analyses have shown that this is indeed the case, although the Cerenkov emission rate is sometimes small—only second order in the relevant Lorentz-violating parameters [99].

The two major areas that this dissertation will address come in two different sectors of the SME. The photon sector for dealing with electromagnetic extensions and the weak sector for the quantum field-theoretic type. Brief summaries of the important aspects are summarized here for each of these published works [48, 22], which are given in chapters 3 and 4.

Before considering the models of specific type developed in this dissertation, we give an example of a Lagrangian with more general symmetry breaking, considered along the lines of the minimal SME, with an example Lagrangian in the fermion sector of the theory. Effectively, this means extending relativistic quantum mechanics in the Standard Model to include nontrivial vector and tensor backgrounds. For a single species of fermions, we have a modified Dirac Lagrange density

$$\mathcal{L} = \bar{\Phi}(\frac{i}{2}\Gamma^{\nu}\overleftrightarrow{\partial_{\nu}} - M)\Phi. \tag{2.1}$$

The Γ and M in the above equation contain possible matrix structures as small corrections that break the Lorentz symmetry. The Lorentz invariant terms in Γ and M are the usual terms from relativistic quantum field theory; γ^{ν} and mass terms m and m_5, which is typically removed by a chiral transformation of the fermion field. All other terms violate Lorentz invariance but not all violate CPT. Thus, we choose M and Γ to be defined as follows,

$$M = m + im_5\gamma_5 + a^{\nu}\gamma_{\nu} + b^{\nu}\gamma_5\gamma_{\nu} + \frac{1}{2}H^{\nu\mu}\sigma_{\nu\mu}, \tag{2.2}$$

$$\Gamma^\nu = \gamma^\nu + c^{\mu\nu}\gamma_\mu + d^{\mu\nu}\gamma_5\gamma_\nu + e^\nu + if^\nu\gamma_5 + \frac{1}{2}g^{\alpha\mu\nu}\sigma_{\alpha\mu}. \tag{2.3}$$

The non-standard terms represent background vectors and tensors, which describe preferred direction structures that exist in the quantum vacuum. The terms in M are of dimension (mass)^1, and the coefficients in Γ are dimensionless. Discrete symmetries of the backgrounds are determined by the C, P and T behaviors of the Dirac matrices they multiply. For example, the time component b_0 multiplies $\gamma_5\gamma_0$, which is odd under P but even under C and T, while the spatial components of b are odd under T but even under C and P. Whether a particular symmetry breaking term also breaks CPT symmetry is largely determined by how many Lorentz indices there are on the tensor; typically only tensors with odd numbers of indices can break CPT Ref. [9].

In the minimal SME, the Lagrange density for the electromagnetic sector is [33, 34]

$$\mathcal{L} = -\frac{1}{4}F^{\mu\nu}F_{\mu\nu} - \frac{1}{4}k_F^{\mu\nu\rho\sigma}F_{\mu\nu}F_{\rho\sigma} + \frac{1}{2}k_{AF}^{\mu}\epsilon_{\mu\nu\rho\sigma}F^{\nu\rho}A^\sigma - j^\mu A_\mu. \tag{2.4}$$

This includes all the superficially renormalizable operators that can be constructed solely out of photon fields. The CPT-even operators are the ones that multiply the nineteen independent $k_F^{\mu\nu\rho\sigma}$ coefficients. Although there are many potentially interesting phenomena that could appear in the presence of nonzero $k_F^{\mu\nu\rho\sigma}$ terms, we shall not be focusing on them here. Instead we shall be looking at possible effects of the four-component (axial vector) k_{AF}^μ term. The associated operators are all CPT odd, and k_{AF}^μ itself has dimension (momentum)^1. Chapter 3 will further review a particularly simple and potentially illuminating radiation process in the modified Maxwell theory—emission by a harmonically oscillating dipole.

Since, in our second model, chapter 4, we shall be focusing on the outgoing kinematics of a three-body decay, with the daughter particles all identical, we shall only need to consider a sector of the minimal SME with a single field. The Lagrange density, which involves the standard mass and kinetic terms from the quantum field theory, as well as our Lorentz-violating background tensor, is

$$\mathcal{L} = \frac{1}{2}(\partial^\mu \pi)(\partial_\mu \pi) + c_{\mu\nu}(\partial^\mu \pi)(\partial^\nu \pi) - \frac{1}{2}m^2\pi^2. \tag{2.5}$$

Here, π is the spinless field of which the three daughter particles are excitations. The coefficients $c_{\mu\nu}$ form a symmetric two-index tensor background, which describes violations of rotation and boost symmetries, but without any breaking of CPT. For a single real Klein-Gordon field, this is the only type of Lorentz violation possible in the minimal SME context.

In order to explain the experimental bounds given in the following section, the theory framework necessary to understand the specific experiments highlighted there is developed in the rest of this section. We turn to the Fold-Wouthuysen transformed non-relativistic Hamiltonian,

$$\delta\mathcal{H} \;=\; c_{(0j)}\, p_j \;+ \left(c_{jk} \;+\; \frac{1}{2}\, c_{00}\, \delta_{jk}\right) \frac{p_j\, p_k}{m}. \tag{2.6}$$

$\delta\mathcal{H}$ represents the terms that would need to be subtracted from the non-relativistic kinetic energy term in the regular Hamiltonian. Of the nine components of the symmetrized tensor $c^{(\mu\nu)}$, the isotropic term c_{00} and the mixed term c_{0j} are not directly observable from this Hamiltonian. Relativistic effects may be observed by comparing observations in two different frames, one boosted relative to the other. The observer in the boosted frame will see the components of $c^{\mu\nu}$ reshuffled, therefore,

the observed isotropic (and thus the apparent inertial mass) will change between the frames. Another possibility could enter under these relativistic effects by a particle-antiparticle annihilation process. With Lorentz violation, the inertial mass observed through the action of nonrelativistic forces does not have to be identical to the rest energy released in an annihilation event.

The maximum attainable velocity (MAV), for an electron or positron, moving in the direction $\hat{p}$ is then

$$\mathcal{V}_{MAV} \;=\; 1 \;-\; c_{00} \;-\, c_{(0j)}\,\hat{p}_j \;-\; c_{jk}\,\hat{p}_j\,\hat{p}_k \tag{2.7}$$

The particle's energy and velocity are thus similar to that in normal special relativity, except that the limiting speed is now $1 + \delta$, instead of just 1, the speed of light. For electrons and other types of particles, the presence or absence of these Lorentz violating processes is used to place bounds or very strong constraints on these parameters. Three different spatial symmetries result directly from (2.7). The time-time component c_{00} gives an isotropic shift in the velocity. Although, the four-tensor $c^{\mu\nu}$ by definition is traceless, so that isotropic breaking of boost symmetry is not actually described by just the c_{00}. The traceless isotropic part of the tensor must contain the diagonal space-space components $c_{jk} \;=\; \frac{1}{3}\,c_{00}\,\delta_{jk}$. Then, the isotropic tensor leads to MAV of $1 \,-\, \frac{4}{3}\,c_{00}$, which may be greater than or less than the speed of light. The mixed components, the time-space components, are given by a three-vector with components $c_{(0j)}$. They give rise to how the speed along a direction of the momentum is slowed down but in the antiparallel direction is sped up; and in oblique directions, the MAV follows a dipolar pattern. The space-space components, from the symmetric, traceless three-tensor, $c_{(jk)} \,-\, \frac{2}{3}\,c_{00}\,\delta_{jk}$, present a quadrupolar change

in the MAV. All nine of these components are physically observable and represent the possible spatial symmetries allowed in a minimal SME. If $\delta < 0$, the energy along the direction of the particle momentum would grow more rapidly with increasing velocity than in conventional relativity. Therefore, processes such as photon decay $\gamma \rightarrow e^- + e^+$ may be allowed. The fact that a photon moving in a source-to-Earth direction can survive long enough to arrive at the laboratory indicates that the process is forbidden for this combination of Energy E and momentum direction $\hat{p}$, or $\delta(\hat{p}) > -2m^2/E^2$.

2.2 Experimental Status

Interest has spiked in the twenty-first century in experimental tests of Lorentz violation. Improving bounds and experiments are important to further our understanding of fundamental physics. When evaluating which theory has the greatest potential for further development, it is a priority to compare experiments. According to the theoretical framework given in the previous section, the SME provides a basis for comparing experimental and theoretical studies of Lorentz violation, including those involving atoms, photons, hadrons, Higgs bosons, and gravity.

In this section, we outline some experimental methods for obtaining bounds on coefficients in the SME. In table 2.1, there are some typical examples of bounds for the terms that we introduce in our models: k^{μ}_{AF} and $c^{\mu\nu}$, in the photon and electron sectors. The $c^{\mu\nu}$ are considered to be some of the most important Lorentz-violating modifications to the standard fermion kinetic term. For kinematic reasons, this two-index tensor is expected to predominate over all other renormalizable forms

of Lorentz violation at ultrarelativistic energies. If this term is nonzero, the limiting velocities of high-energy particles need not be the same as the speed of light, while other terms in the minimal SME Lagrangian do not affect the MAV. Because the photon survival bounds do not depend on how the photons are produced, these bounds are the cleanest for the high-energy astrophysical bounds on the electron $c^{\mu\nu}$ coefficients. To constrain all nine of the $c^{\mu\nu}$ coefficients, observations of radiation approaching from many different momentum directions are used.

More up-to-date bounds on the SME coefficients may be found in Ref. [105]. The electromagnetic sector of the SME contains terms that depend on photon polarization. These terms are measurable by astrophysical polarimetry [100, 101]. Any dependence of polarization on the phase speed of light will lead to birefringence–a change in the polarization of light waves as they propagate [15]. The term in the minimal SME action that produce vacuum birefringence have been tightly bounded using polarimetric data from cosmologically-distant sources. For the four components of k^{μ}_{AF}, which give rise to wavelength-independent rotations in the planes of polarization of initially linear-polarized waves and parity-violating correlations in the polarization of the cosmic microwave background (CMB), the bounds have been placed at the 10^{-44} GeV level or better, beginning with Ref. [91] for quasar jets and more recently using CMB data [62]. Of the nineteen independent coefficients in $k_F^{\mu\nu\rho\sigma}$, ten of them also generate photon birefringence, and they are also quite tightly constrained, at the 10^{-34}–10^{-38} [37, 102, 82] levels. On the other hand, the remaining nine coefficients from $k_F^{\mu\nu\rho\sigma}$ are much more difficult to measure, and precision optical experiments and astrophysical data have been used to bound them

only at 10^{-14}–10^{-22} levels [108, 104, 38]. However, this last group of parameters, the nonbirefringent ones that are the most challenging to measure directly, actually have effects on dipole radiation that are already completely understood, since they may actually be eliminated from the photon sector entirely by means of an oblique linear transformation of the spacetime coordinates.

The SME provides the framework for applying an experimental test of Lorentz and CPT symmetry. Sensitive searches include studies of matter-antimatter asymmetries for trapped charged particles [78] and bound state systems [79], determinations of muon properties [76], analyses of the behavior of spin-polarized matter [77], frequency standard comparisons [61], Michelson-Morely experiments with cryogenic resonators [8], Doppler effect measurements [65], measurements on the light from distant galaxies [28, 100, 103, 101], high energy astrophysical tests [95, 97, 16, 12], and more. The results of these experiments set the bounds on many SME coefficients.

Sector	Coefficient	Sensitivity	System	Ref.
Photon	$k^{(3)}_{(V)00}$	$1.54 \cdot 10^{-44}$ GeV	CMB polarization	[28]
"	$k^{(3)}_{(V)10}$	$16 \cdot 10^{-21}$ GeV	Schumann resonances	[70]
"	$k^{(3)}_{(V)11}$	$12 \cdot 10^{-21}$ GeV	"	[71]
"	k_{AF}	$7.4 \cdot 10^{-45}$ GeV	CMB polarization	[63]
"	k_{AF}	$1.03 \cdot 10^{-26}$ GeV	Satellites	[4]
	$k^{(3)}_{AF}$	$(0.57 \pm 0.70) H_0$	Astrophysical Birefringence	[28]
Electron	c_{00}	(-1.6 to 0.000019)$\cdot 10^{-14}$	Combined	[2]
"	c_{x-y}	$(-5.2 \pm 7.8) \cdot 10^{-21}$	Trapped Yb ion	[64]
Electroweak	$(k_{\phi\phi})^{XT}_S$	$3.3 \cdot 10^{-3}$	Kaon decay	[7]
"	$(k_{\phi\phi})^{YT}_S$	$6.3 \cdot 10^{-3}$	"	"

Table 2.1 The table represents the experimental bounds for the coefficients used in our models developed in chapters 3 and 4

In the weak interaction sector, there are possibilities to study Lorentz violation in non-leptonic decays. This is to what we study in chapter 4, except that the Lorentz violation effect enters through the addition of a tensor $\chi^{\mu\nu}$ to the W-boson propagator. The framework for this bounding method can be found in [7]. In their kaon decay experiment the KLOE collaboration looked at the directional dependence of the lifetime of the neutral kaon.

We briefly review methods for these experimental tests, for backgrounds tensors that rotate with the Earth. Earth-based laboratories will see slightly different local physics as the planet rotates. The general idea is to create a system such as an atomic clock that according to Standard Model physics continues to tick at a constant rate. It is then monitored as it rotates with the Earth through the preferred direction background field. If it speeds up and slows down in correlation with its orientation, then it has provided evidence of a Lorentz violation. Since these are background fields, if, for example, a pendulum is affected by Lorentz violating anisotropy effects, then its behavior from a given time will be identical to its behavior after one sidereal day has passed—but not identical for a (slightly longer) solar day. For these types of tests, the components of the background, as observed in the lab frame, vary in time t with the periodicity of the Earth's sidereal rotation frequency $\Omega = \frac{2\pi}{23\mathrm{h}\,56\mathrm{m}}$. Clock comparison tests of this type typically bound the amplitude of the time variation of a transition frequency, which is related to the difference between energy levels. To determine the time dependence of the energy levels in terms of the Lorentz violating parameters, in a more general situation one would apply the Euler rotations to each component to transform them into a non-rotating frame—going from the rotating

frame (x, y, z) to the Sun-centered frame (X, Y, Z) in which SME bounds are typically reported.

However, some newer experiments are using actively rotating apparatuses. The reason for doing so is that Earth's motion may prevent us from measuring certain quantities. This brings added sensitivity to a preferred direction parallel to Earth's rotation axis. One possible experiment is to use an upgraded Michelson-Morely technique. With laser beams propagating in vacuum, this can only be sensitive to the photon sector unless the resonant cavity is matter-filled, making the length of the cavity change as the device is rotated [9]. The trapped Yb^+ experiment in the table from Ref. [64], they search for Lorentz violation by comparing atomic orbitals in similar modified version of a Michelson-Morely experiment.

Chapter 3

Title of Manuscript:

Radiation from an Oscillating Dipole in the Presence of Photon-Sector CPT and Lorentz Violation

[1]

[1] J. O'Connor and B. Altschul, Physical Review D **109** 045005, 1-12, 5 Febuary 2024, Published

3.1 Outline

The work in this chapter has been published in Ref. [48]. The sections of chapter 3 are ordered as follows. In section 3.2, we describe the model of Lorentz-violating electrodynamics with a CPT-odd Chern-Simons term. In this theory, the free propagation models of the electromagnetic field exhibit vacuum birefringence. Taking what is known about these plane wave modes, we determine the lowest-order modifications to the radiation-zone fields of an oscillating dipole in section 3.3 and evaluate the standard Poynting vector $\vec{S}^{(0)} = \vec{E} \times \vec{B}^{\,*}$ with the modified fields. The formalism and computational details are outlined and analyzed for the ultimate goal of finding a modification to the classical electrodynamic Larmor expression for the total power radiated. In classical electrodynamics, the conservation of energy and momentum must be preserved. We state the continuity equation; the time rate of change within a certain volume, plus the energy flowing out through the boundary surfaces of the volume per unit time, is equal to the negative of the total work done by the fields on the source within the volume. We consider emission of radiation by localized systems of harmonically oscillating charge where the sources are sufficiently simple that direct evaluation of the radiation field is easy. The sources are localized in an otherwise empty space. For a localized system, we use Fourier analysis to handle each Fourier component independently. We can therefore define a localized system of charges and currents that vary sinusoidally in time. Charge and current density; with the position dependence multiplied by $e^{i\omega t}$, we take the real part of the expressions to obtain physical quantities. Thus, the fields have the same time dependence. Then, in non-modified theory, the flow of energy is described by the Complex Poynt-

ing vector which becomes modified by the Chern Simons parameter in our model. The real part of the Poynting vector which is also modified by the Chern-Simons parameter is the instantaneous flux of energy in units ($energy/area \times time$). In our extended theory and in the regular classical electrodynamics case, the electric and magnetic fields remain transverse and perpendicular. The transverse component of S represents the reactive energy flow and does not contribute to the time- averaged flux of energy. Otherwise, to evaluate the total power flow $\mathcal{P}$, we integrate the axial component of S over the area of the cross section A. The total power in non-modified theory (the Larmor expression), by a harmonically oscillating dipole is

$$\mathcal{P} = \int d\Omega \, r^2 \, \vec{n} \cdot \, \vec{S}^{(0)} = \frac{c^2 \, Z_0 \, k^4}{12\pi} \, |\vec{p}|^2 \tag{3.1}$$

Furthermore, in section 3.4, we look at two additional ways in which the energy and momentum emission may be modified, which were not captured by the first set of calculations. Finally, section 3.5 presents our conclusions and the outlook for further extensions of this work.

3.2 CPT- and Lorentz-Violating Electrodynamics

Radiation spectra are already modified at second order in the magnitude of a Lorentz-violating Chern-Simons term in the photon sector. If effects for evaluating the classical dipole radiation and another standard radiation process were found at leading order, this could lead to new physical conclusions about the phenomenalistic viability of the theory. Further, analyses of uniform radiation processes allow us to identify novel effects, such as the self-force on an accelerated charge. The Maxwell-Chern-

Simons Lagrange density is used to describe the theory. The Lagrangian contains two four component axial vectors which are CPT-even and CPT-odd photon field operators. We can truncate the minimal SME to minimal Lorentz and CPT-violating extension to include a U(1) gauge invariant Lagrangian and consider the CPT-odd Chern-Simons term. The change to the field equations can be viewed as a field dependent addition to the source current. The modified classical dispersion relation for a plane wave solution implies that the wave will be rotated when it travels through space, based on the two polarization modes. The modified polarization vectors are calculated, and it is found that the magnetic field and the electric field are allowed to have different elliptical polarizations. The polarization leads to changes in the modified electromagnetic components of the energy-momentum tensor; however, these changes are unphysical. Only physically meaningful quantities are the energy and momentum density integrated over all space. There is a divergence of the energy density in the time-like theory. The energy instability can be dealt with by the preferred frame or by selecting an acausal Greens function.

While a completely new effect that can only occur because of Lorentz violation (such as vacuum Cerenkov radiation when boost symmetry is broken, or a transition between two states with different angular momentum values in a theory with broken rotation symmetry) will typically appear at second order in the symmetry-breaking interaction coefficients, modifications to phenomena that already occur in the standard theory can be observable at lower order—for example, as small interference effects on top of conventional observables. Our approach in this chapter will be to look for a modification of this nature—a change to the conventional Larmor expression

for the energy-momentum radiated by a harmonically oscillating dipole. Radiation spectra are known to be substantially and nonperturbatively modified at second order in the magnitude of a Lorentz-violating Chern-Simons term in the photon sector. However, by looking for modifications to standard dipole radiation, we open up the possibility of finding observable changes already at first order. Dipole radiation also provides an extremely clean theoretical laboratory for identifying novel behavior. For example, radiation damping is typically a very awkward topic in classical electrodynamics; however, for the dipole source created by a harmonically oscillating charge, it is possible to define a radiative friction term which (so long as the radiation is not too rapid) avoids most of the awkwardness that typically accompanies the evaluation of the self-force on an accelerated charge.

In contrast, although they have already been extremely well constrained by polarimetry as shown in section 2.2, the CPT-odd k^{μ}_{AF} terms are still of interest for theoretical, but also potentially practical, reasons. From its first introduction, there have been questions about whether it is even possible to have a nonzero k^{μ}_{AF} in a consistent field theory, and so far there have been conflicting indications [91, 99, 56, 89]. The theory with just the Chern-Simons term does not appear to be energetically stable, even classically, and there were concerns about whether it was even possible for such a theory to have a well-defined, unitary S-matrix—which is a fairly basic requirement for a physically meaningful theory. One obvious way that such an inconsistency might manifest itself would be through runaway vacuum Cerenkov radiation, because the Chern-Simons theory contains arbitrarily slow phase speeds. In fact, any radiation process might potentially be subject to unstable, nonperturbative

behavior that might invalidate the theory, so studying standard radiation scenarios in the presence of the Chern-Simons term could potentially lead us to new physical conclusions about the phenomenalistic viability of the theory. This is one of the key motivations for this work. Moreover, questions about whether the structure of the Chern-Simons term could make a k^{μ}_{AF} theory mathematically or physically inconsistent are actually fairly reasonable, in light of its unusual structural properties. The term's structure means that potential radiative corrections to the photon k^{μ}_{AF} must come from virtual processes that are extremely similar to those that appear in chiral anomaly triangle diagrams [84, 29, 75], and the cancellation of the related gauge anomalies is already known to give nontrivial restrictions on the structure of internally consistent quantum field theories.

For brevity, we shall drop the "AF" labels and henceforth write $k^{\mu}_{AF} = k^{\mu}$. With the Chern-Simons term present, the purely electromagnetic part of the energy-momentum tensor becomes [91]

$$\Theta^{\mu\nu} = -F^{\mu\alpha}F^{\nu}{}_{\alpha} + \frac{1}{4}g^{\mu\nu}F^{\alpha\beta}F_{\alpha\beta} - \frac{1}{2}k^{\nu}\epsilon^{\mu\alpha\beta\gamma}F_{\beta\gamma}A_{\alpha}. \tag{3.2}$$

The tensor is not symmetric, and the asymmetry is in fact a measure of the Lorentz violation. The main terms of interest are the energy density ($\mathcal{E} = \Theta^{00}$), energy flux ($S_j = \Theta^{j0}$), and momentum density ($\mathcal{P}_j = \Theta^{0j}$),

$$\mathcal{E} = \frac{1}{2}\vec{E}^2 + \frac{1}{2}\vec{B}^2 - k_0\vec{A}\cdot\vec{B} \equiv \mathcal{E}^{(0)} - k_0\vec{A}\cdot\vec{B} \tag{3.3}$$

$$\vec{S} = \vec{E}\times\vec{B} - k_0A_0\vec{B} + k_0\vec{A}\times\vec{E} \equiv \vec{S}^{(0)} - k_0A_0\vec{B} + k_0\vec{A}\times\vec{E} \tag{3.4}$$

$$\vec{\mathcal{P}} = \vec{E}\times\vec{B} - \vec{k}\left(\vec{A}\cdot\vec{B}\right) \equiv \vec{S}^{(0)} - \vec{k}\left(\vec{A}\cdot\vec{B}\right), \tag{3.5}$$

in terms of the time and space components of $k^{\mu} = (k_0, \vec{k}\,)$. Note that none of these

quantities are gauge invariant, because they depend not just on the field strengths $\vec{E}$ and $\vec{B}$, but also on the scalar and vector potentials. However, the total energy and total momentum, found by integrating $\mathcal{E}$ and $\vec{\mathcal{P}}$ over all space, are gauge invariant. This is not necessarily obvious from the forms of these densities, but the key property is that $\mathcal{E}$ and $\vec{\mathcal{P}}$ (and also the Lagrange density $\mathcal{L}$) change under gauge transformations by terms that are total derivatives, and which thus make no contributions to the integrated quantities.

The form of the energy density exhibits one of the elements that makes the analysis of this theory somewhat tricky—that the energy is not bounded below. The $-k_0\vec{A}\cdot\vec{B}$ term may be made arbitrarily negative by increasing the magnitude of the field $\vec{A}$ (and thus simultaneously increasing the magnitude of $\vec{B}=\vec{\nabla}\times\vec{A}$). For modes of the field with sufficiently long wavelengths, the $-k_0\vec{A}\cdot\vec{B}$ in $\mathcal{E}$ will win out over the usual $\frac{1}{2}\vec{B}^2$. This downward unboundedness of the the energy also has a manifestation in the plane wave dispersion relations. If k^μ is purely timelike, meaning $\vec{k}=0$, the (birefringent) dispersion relation is $\omega_\pm^2 = Q(Q\pm 2k_0)$, for waves with wave vector $\vec{Q}$ and positive and negative helicities, respectively. This is a special case of (3.11) below, and it identifies the Fourier modes with $Q<2|k_0|$ as precisely those for which instabilities may occur. For these modes, the time dependence may be exponentially growing, rather than oscillatory. This kind of runaway growth is "powered" by the ever-decreasing energy of the $-k_0\vec{A}\cdot\vec{B}$ term in $\mathcal{E}$.

These runaway modes do not necessarily have to ruin the Chern-Simons theory with timelike k^μ, but they certainly do raise significant questions. It is possible to avoid the instability by giving up causality. The Green's functions for the theory

may be chosen such that the exponentially growing modes are never populated, but the cost is having solutions in which charged sources will begin to radiate before they actually begin to move [91]. The acausality is relatively weak so long as k_0 is small, so that using the acausal Green's functions to describe the emission of long radio-frequency wave trains is probably unproblematic. However, it remains unclear whether, at a more fundamental level, it is physically sensible to have a theory with these kinds of acausal behavior. Perhaps even more strangely, the modes with $Q < 2|k_0|$ actually seem to rescue the timelike Chern-Simons theory from other kinds of instability, rather than causing it! Any photon dispersion relation for with $\omega/Q < 1$ opens up the possibility of Cerenkov radiation. Conventional Cerenkov radiation is a phenomenon that occurs in material media, in which the phase speed of light is slowed down. When charged particles move through faster than the in-medium ω/Q, they emit a burst of radiation, analogous to masses moving faster than the speed of sound in a fluid produce sonic booms. Since the real branch of the Chern-Simons dispersion relation $\omega^2 = Q(Q-2|k_0|)$ extends all the way down to $\omega = 0$, any moving charge with speed v is going to outpace some of the propagating electromagnetic field modes, no matter how small v is. A natural expectation (based on phase space availability considerations [13]) would therefore be that any charge in uniform motion would lose energy to vacuum Cerenkov radiation, until it came to rest in the frame were $\vec{k} = \vec{0}$. However, this turns out not to be case, for the following subtle reason [56, 18, 80]. Modes of the field with $2|k_0| < Q < 2|k_0|/(1-v^2)$ do carry power away, but the modes with $Q < 2|k_0|$ actually carry away negative power, in an amount that exactly cancels the net positive emission. For the fields following a

charged particle in uniform motion, the $\omega^2 < 0$ modes are actually associated with propagating solutions carrying negative energies. The result is that in the timelike Chern-Simons theory, just as in standard electrodynamics, charges in uniform motion lose no net energy via radiation.

The theory with a spacelike Chern-Simons four-vector k^μ is potentially better behaved than the timelike theory, but it has other, closely related, peculiarities. The energy instability, which is unavoidable if k^μ is timelike, instead depends on the choice of frame. In particular, there is only an obvious vacuum state, with the energy density function $\mathcal{E}$ bounded from below, in the k_0 reference frame. Analyzing the theory in this preferred frame (including potentially quantizing it) looks like it may be relatively unproblematic, but this leaves open the question of how the theory should be quantized in a different frame, in which the $-k_0\vec{A}\cdot\vec{B}$ term in $\mathcal{E}$ is present. The existence of the particular frame in which the the theory is manifestly stable energetically actually has important implications for the vacuum Cerenkov radiation in the spacelike theory. Once again, a charged particle with a constant velocity $\vec{v}$ may emit radiation. This radiation tends to damp out the motion, until the charge is at rest in the frame where k^μ has no temporal component [85]. This is a remarkable explicit connection between the energetic stability condition and the dynamics of individual charges, and this connection was a very important motivation for the current work.

Understanding radiation processes in the Chern-Simons theory is tricky, and there have already been a number of different innovative approaches. For the timelike theory, the original derivation of the acausal Green's functions was a major step, since

it showed that there were systems that obeyed the equations of motion and emitted radiation, without the amplitudes of long-wavelength modes growing uncontrollably. However, the acausality was an obvious drawback. Looking specifically at the vacuum Cerenkov radiation emitted by a charge in uniform motion provided one way out of this dilemma. If the electromagnetic field, including the radiation component, is moving along in synchronization with the source charge, the time dependences of the field components can be inferred from their spatial profiles at a fixed time, leaving no room of runaway behavior. Considering only versions of the theory with spacelike k^μ also eliminates the obvious stability problem, but only in one frame, and the radiation rate calculated in Ref. [85] takes an extremely unusual and manifestly nonperturbative form—meaning that the effect cannot be found by expanding the theory in powers of the space and time components of the background four-vector k^μ. Instead, the rate of momentum emission via the vacuum Cerenkov radiation coming from a stationary charge is proportional to $-k_0\vec{k}|k_0|^3/|\vec{k}|^3$. (However, in contrast, in the presence of the other types of Lorentz violation, vacuum Cerenkov radiation is more typically a threshold effect, as it is in matter [17, 31])

When investigating a modified version of a generally well-understood theory, looking at modifications to effects that are permitted in the standard theory can, in many cases, be more fruitful than studying entirely new phenomena. Vacuum Cerenkov radiation would be a strikingly novel phenomenon if it were ever to be observed, but the emission rate may be very small. In the spacelike k^μ theory, the spontaneous force—something which does not exist at all in conventional electrodynamics—is of $\mathcal{O}\left(k_0^4/\vec{k}^2\right)$. This work was, in part, an outgrowth of the hope that by looking at a

different radiation process—one which does exist in standard electrodynamics—we might uncover qualitatively similar radiation effects, but that the mathematical descriptions of the modified radiation could be found by expanding all quantities to leading order in k^μ.

We shall therefore consider the radiation emitted by a very simple system—a harmonically oscillating electric dipole $\vec{p}$. There are several different ways of expressing the charge and current densities of a radiating source in terms of sums (or integrals) of simple basis functions. Thanks to the linearity of electrodynamics, the resulting electromagnetic fields will be coherent sums of the fields produced by just the basis functions. For example, the radiation fields generated by an accelerated charge may be written as integrals of the radiation fields (with kinked electric and magnetic field lines) produced by instantaneous impulsive accelerations. However, this method would probably be inapt in the general Chern-Simons theory theory, because it provides no evident way to control the excitation of unstable long-wavelength modes. In contrast, a description of the sources and fields using a Fourier transform in the time domain deals with the problem quite neatly. By working with a source that is excited solely at a frequency ω, we can be assured that no modes with other time dependences will be excited. Moreover, the presence of ω serves another mathematical purpose. In the analyses of vacuum Cerenkov radiation, the only physical quantities on which the radiation rate can depend are the charge q, its velocity $\vec{v}$ (both dimensionless), and the Lorentz-violating k^μ, which has units of (momentum)^1. Since the power emitted has units of (momentum)^2, it must—for dimensional reasons alone—be a homogeneous function of degree two of the components of k^μ. It is simply not

possible to have an effect that appears at perturbative $\mathcal{O}(k)$. However, with the oscillating dipole, there are additional dimensional quantities involved. Multipole moments have units of (momentum)$^{-\ell}$, but ω has units of positive (momentum)^1. That makes it possible to have radiation emission effects at only linear order in k^μ. The standard radiation fields may mix with the k^μ-modified fields to produce correction terms of $\mathcal{O}(k\omega^3)$.

So for our source, we shall take an oscillating electric dipole at the origin and extrapolate its fields outwards into the radiation zone. At very short distances, the sources on the right-hand side of the modified Gauss's law

$$\vec{\nabla} \cdot \vec{E} = \rho + 2\vec{k} \cdot \vec{B} \tag{3.6}$$

are dominated by the conventional term, since the charge density ρ has a strong singularity, $\rho = -\vec{p} \cdot \vec{\nabla}\delta^3(\vec{r})$; and similarly for the modified Ampére-Maxwell law,

$$\vec{\nabla} \times \vec{B} - \frac{\partial \vec{E}}{\partial t} = \vec{J} + 2k_0\vec{B} - 2\vec{k} \times \vec{E}, \tag{3.7}$$

where the singular current distribution of the oscillating dipole dominates the right-hand side in the immediate vicinity of the dipole.

A key consequence of this is that we may use the standard forms for the oscillating fields at infinitesimally short distances from the origin, then propagate them out to larger radii using the known propagation characteristics of the Chern-Simons theory. This takes advantage of the fact that the Fourier spectrum of the propagating modes is well known. Meanwhile we shall, whenever it is convenient, neglect any near-field terms that fall off too rapidly with distance to contribute to the energy and momentum flows at large distances. We shall also take k^μ to be small, so that we

never need consider terms beyond first order in the components of k—except when they are multiplied by a large distance r. This last caveat is necessary because we are interested in the behavior of the fields at arbitrarily large distances. Note also that additional care may be specifically needed for waves propagating in a direction $\hat{r}$ for which $k^\mu \hat{r}_\mu \equiv k_0 - \vec{k} \cdot \hat{r} \approx 0$, since the normal mode polarization vectors may be significantly modified in these angular regions.

3.3 Radiation Fields Modified by k^μ

The standard far-field form for the magnetic field of the oscillating dipole with complexified amplitude $\vec{p}(t) = \vec{p}\, e^{-i\omega t}$ is

$$\vec{B} = \frac{\omega^2}{4\pi} \left(\hat{r} \times \vec{p}\right) \frac{e^{i\omega(r-t)}}{r}. \tag{3.8}$$

To find the version of this in the Chern-Simons theory, it suffices to calculate the projection of this field along the polarization eigenvectors of the modified theory and to attach to each projections a modified propagation factor $e^{i(Qr-\omega t)}$. When the Chern-Simons vector is purely timelike, $k^\mu = (k_0, \vec{0}\,)$, the polarization vectors for the normal modes of propagation are circular,

$$\hat{\epsilon}_\pm = \frac{1}{\sqrt{2}} \left(\hat{\theta} \pm i\hat{\phi}\right). \tag{3.9}$$

When k^μ has spatial components as well, these are still very close to the exact polarization vectors, differing only meaningfully around $k^\mu \hat{r}_\mu \approx 0$. To leading order, the wave numbers corresponding to these circular polarization modes are

$$Q_\pm = \omega \pm k^\mu \hat{r}_\mu = \omega \pm \left(k_0 - \vec{k} \cdot \hat{r}\right). \tag{3.10}$$

This is the leading approximation to the exact (but implicit) relationship between frequency and wave vector [91]

$$\omega^2 - Q_\pm^2 = \mp 2\left[k_0 Q_\pm - \left(\vec{k}\cdot\hat{r}\right)\omega\right]\left(1 - \frac{4\left|\vec{k}\times\hat{Q}\right|^2}{\omega^2 - Q_\pm^2}\right)^{-1/2}. \tag{3.11}$$

With the leading order $Q_\pm$, the propagating part of the magnetic field in the Lorentz-violating theory must be

$$\vec{B} = \frac{\omega^2}{4\pi}\frac{e^{i\omega(r-t)}}{r}\sum_\pm \left[\hat{\epsilon}_\pm^*\cdot\left(\hat{r}\times\vec{p}\right)\right] e^{\pm i\left(k_0 r - \vec{k}\cdot\vec{r}\right)}\,\hat{\epsilon}_\pm \tag{3.12}$$

(with the sum referring to the sum over the $\pm$ modes).

We shall select a coordinate system so that oscillating dipole lies in the xy-plane,

$$\vec{p} = p_x\,\hat{x} + p_y\,\hat{y} = p_1\,\hat{x} + e^{i\alpha}p_2\,\hat{y}, \tag{3.13}$$

where p_1, p_2, and α are real quantities. Although the components p_x and p_y would generally be complex, we have taken advantage of the fact that we can shift the overall phase (either by a redefinition of the zero of t or by a rotation of the xy-plane) to make the quadrature component along the x-direction real. It will also be convenient to have a separation of the oscillating dipole moment into its phase components—that is, its real and imaginary parts,

$$\vec{p} = \vec{p}_R + i\vec{p}_I. \tag{3.14}$$

Then the necessary triple products are

$$\hat{\epsilon}_\pm^*\cdot(\hat{r}\times\vec{p}) = \frac{1}{\sqrt{2}}\left(\hat{\theta}\mp i\hat{\phi}\right)\cdot\Big[\left(p_1\sin\phi - e^{i\alpha}p_2\cos\phi\right)\hat{\theta} + \left(p_1\cos\phi + e^{i\alpha}p_2\sin\phi\right)\cos\theta\,\hat{\phi}\Big], \tag{3.15}$$

so that the expressions for the full summand terms are

$$\begin{aligned}\left[\hat{\epsilon}_{\pm}^{*}\cdot\left(\hat{r}\times\vec{p}\right)\right]e^{\pm i\left(k_0 r-\vec{k}\cdot\vec{r}\right)}\,\hat{\epsilon}_{\pm} &= \frac{1}{2}\Big(p_1\sin\phi - e^{i\alpha}p_2\cos\phi \mp ip_1\cos\theta\cos\phi \\ &\quad \mp ie^{i\alpha}p_2\cos\theta\sin\phi\Big)\,e^{\pm i\left(k_0 r-\vec{k}\cdot\vec{r}\right)}\left(\hat{\theta}\pm i\hat{\phi}\right). \quad (3.16)\end{aligned}$$

Note that the two terms (corresponding to $\pm$ subscripts) are almost complex conjugates, except that the $e^{i\alpha}$ factors are unchanged between the two. Thus it will be convenient to write the expressions in the forms

$$\left[\hat{\epsilon}_{+}^{*}\cdot\left(\hat{r}\times\vec{p}\right)\right]e^{+i\left(k_0 r-\vec{k}\cdot\vec{r}\right)}\,\hat{\epsilon}_{+} = \frac{1}{2}\left(\mathcal{A}_1\,\hat{\theta}+i\mathcal{A}_1\,\hat{\phi}+e^{i\alpha}\mathcal{A}_2\,\hat{\theta}+ie^{i\alpha}\mathcal{A}_2\,\hat{\phi}\right) \quad (3.17)$$

$$\left[\hat{\epsilon}_{-}^{*}\cdot\left(\hat{r}\times\vec{p}\right)\right]e^{-i\left(k_0 r-\vec{k}\cdot\vec{r}\right)}\,\hat{\epsilon}_{-} = \frac{1}{2}\left(\mathcal{A}_1^{*}\,\hat{\theta}-i\mathcal{A}_1^{*}\,\hat{\phi}+e^{i\alpha}\mathcal{A}_2^{*}\,\hat{\theta}-ie^{i\alpha}\mathcal{A}_2^{*}\,\hat{\phi}\right), \quad (3.18)$$

where $\mathcal{A}_1$ and $\mathcal{A}_2$ are

$$\begin{aligned}\mathcal{A}_1 &= p_1\left(\sin\phi - i\cos\theta\cos\phi\right)\left[\cos\left(k_0 r-\vec{k}\cdot\vec{r}\right)+i\sin\left(k_0 r-\vec{k}\cdot\vec{r}\right)\right] \quad (3.19)\\ &= p_1\Big\{\left[\sin\phi\cos\left(k_0 r-\vec{k}\cdot\vec{r}\right)+\cos\theta\cos\phi\sin\left(k_0 r-\vec{k}\cdot\vec{r}\right)\right] \\ &\quad - i\left[\cos\theta\cos\phi\cos\left(k_0 r-\vec{k}\cdot\vec{r}\right)-\sin\phi\sin\left(k_0 r-\vec{k}\cdot\vec{r}\right)\right]\Big\} \quad (3.20)\\ \mathcal{A}_2 &= -p_2\left(\cos\phi + i\cos\theta\sin\phi\right)\left[\cos\left(k_0 r-\vec{k}\cdot\vec{r}\right)+i\sin\left(k_0 r-\vec{k}\cdot\vec{r}\right)\right] \quad (3.21)\\ &= p_2\Big\{\left[-\cos\phi\cos\left(k_0 r-\vec{k}\cdot\vec{r}\right)+\cos\theta\sin\phi\sin\left(k_0 r-\vec{k}\cdot\vec{r}\right)\right] \\ &\quad - i\left[\cos\theta\sin\phi\cos\left(k_0 r-\vec{k}\cdot\vec{r}\right)+\cos\phi\sin\left(k_0 r-\vec{k}\cdot\vec{r}\right)\right]\Big\}. \quad (3.22)\end{aligned}$$

For a linear dipole, $\alpha = 0$, these expressions reduce to a familiar birefringent form. The θ-component of the magnetic field is proportional to $\Re\left\{\mathcal{A}_1+\mathcal{A}_2\right\}$, or

$$\begin{aligned}B_\theta &\propto \left(p_1\sin\phi - p_2\cos\phi\right)\cos\left(k_0 r-\vec{k}\cdot\vec{r}\right) \\ &\quad +\left(p_1\cos\phi+p_2\sin\phi\right)\cos\theta\sin\left(k_0 r-\vec{k}\cdot\vec{r}\right) \quad (3.23)\\ &\propto \cos\left\{\left(k_0 r-\vec{k}\cdot\vec{r}\right)-\tan^{-1}\left[\frac{\left(p_1\cos\phi+p_2\sin\phi\right)\cos\theta}{p_1\sin\phi-p_2\cos\phi}\right]\right\}. \quad (3.24)\end{aligned}$$

Similarly, the ϕ-component may be seen to be proportional in the same fashion to the the imaginary part,

$$\begin{aligned} B_\phi &\propto (p_1 \sin\phi - p_2 \cos\phi) \sin\left(k_0 r - \vec{k}\cdot\vec{r}\right) \\ &\quad -(p_1 \cos\phi + p_2 \sin\phi)\cos\theta \cos\left(k_0 r - \vec{k}\cdot\vec{r}\right) \qquad (3.25) \\ &\propto \sin\left\{\left(k_0 r - \vec{k}\cdot\vec{r}\right) - \tan^{-1}\left[\frac{(p_1\cos\phi + p_2\sin\phi)\cos\theta}{p_1\sin\phi - p_2\cos\phi}\right]\right\}. \qquad (3.26) \end{aligned}$$

This shows a linearly polarized field of constant amplitude $\left|\vec{B}\right|$, but with a polarization direction that is corkscrewing around the propagation direction $\hat{r}$. This effect has been used as the basis for placing extremely tight constraints on the components of the physical k^μ coefficients [91, 90, 100, 103]. The phase constant in (3.24) and (3.26) is independent of the radius. It depends only on the oscillating dipole $\vec{p}$ and the angles (θ, ϕ) that describe the radiation direction. The quantities $p_1\cos\phi + p_2\sin\phi$ and $p_1\sin\phi - p_2\cos\phi$ are the projections of $\vec{p}$ parallel and perpendicular to the axial direction $\hat{\rho}$, and the former appears with the geometrical foreshortening factor $\cos\theta$. Obviously, the same holds for the amplitude of the local magnetic field oscillations, which is proportional to the square root of

$$(p_1\cos\phi + p_2\sin\phi)^2\cos^2\theta + (p_1\sin\phi - p_2\cos\phi)^2 = \vec{p}^{\,2} - (\vec{p}\cdot\hat{r})^2, \qquad (3.27)$$

although for this quantity the dependence on the projections of $\vec{p}$ is a well-known feature of the standard theory.

To the extent that the polarization vectors are accurately represented by (3.9) in the Chern-Simons theory, it continues to be the case that the plane wave propagating modes of the theory have electric and magnetic components related by $\vec{E} = \vec{B}\times\hat{r}$, so that $E_\theta = B_\phi$ and $E_\phi = -B_\theta$. The effect of k^μ is to cause the electric field direction

to revolve in the same way as the magnetic field direction, while $\vec{E}$ and $\vec{B}$ remain transverse and perpendicular. Therefore, the radial component of the unmodified expression for the Poynting vector when the source dipole $\vec{p}$ is linearly polarized is

$$\vec{S}^{(0)} \cdot \hat{r} = \frac{1}{2} \Re \left\{ \vec{E} \times \vec{B}^* \right\} \cdot \hat{r} = \frac{1}{2} \Re \left\{ B_\theta B_\theta^* + B_\phi B_\phi^* \right\}, \tag{3.28}$$

which—as is evident from (3.24) and (3.26)—is unchanged from the value taken in conventional, Lorentz-invariant electrodynamics.

However, things may become significantly trickier when the dipole is oscillating elliptically. In (3.23–3.26), the magnetic field amplitudes [with $e^{i\omega(r-t)}$ factored out] reduced to real expressions, but this will not be true in the presence of a nonzero α. Instead of p_2, $e^{i\alpha} p_2 = p_2(\cos\alpha + i \sin\alpha)$ always appears. Reading off, by analogy with (3.23–3.26),

$$\begin{aligned} B_\theta \;\propto\; & \left[(p_1 \cos\phi + p_2 \cos\alpha \sin\phi)^2 \cos^2\theta + (p_1 \sin\phi - p_2 \cos\alpha \cos\phi)^2 \right]^{1/2} \\ & \times \cos\left\{ \left(k_0 r - \vec{k} \cdot \vec{r} \right) - \tan^{-1} \left[\frac{(p_1 \cos\phi + p_2 \cos\alpha \sin\phi) \cos\theta}{p_1 \sin\phi - p_2 \cos\alpha \cos\phi} \right] \right\} \\ & - i p_2 \sin\alpha \left[\cos\phi \cos\left(k_0 r - \vec{k} \cdot \vec{r} \right) - \cos\theta \sin\phi \sin\left(k_0 r - \vec{k} \cdot \vec{r} \right) \right] \end{aligned} \tag{3.29}$$

$$\begin{aligned} B_\phi \;\propto\; & \left[(p_1 \cos\phi + p_2 \cos\alpha \sin\phi)^2 \cos^2\theta + (p_1 \sin\phi - p_2 \cos\alpha \cos\phi)^2 \right]^{1/2} \\ & \times \sin\left\{ \left(k_0 r - \vec{k} \cdot \vec{r} \right) - \tan^{-1} \left[\frac{(p_1 \cos\phi + p_2 \cos\alpha \sin\phi) \cos\theta}{p_1 \sin\phi - p_2 \cos\alpha \cos\phi} \right] \right\} \\ & - i p_2 \sin\alpha \left[\cos\phi \sin\left(k_0 r - \vec{k} \cdot \vec{r} \right) + \cos\theta \sin\phi \cos\left(k_0 r - \vec{k} \cdot \vec{r} \right) \right], \end{aligned} \tag{3.30}$$

the real parts of these expression are still straightforward; however, one more set of trigonometric identities are necessary to simplify the imaginary parts. The amplitudes of the imaginary parts of (3.29) and (3.30) are

$$p_2 \sin\alpha \left(\cos^2\phi + \cos^2\theta \sin^2\phi \right)^{1/2} = \left[\vec{p}_I^{\,2} - (\vec{p}_I \cdot \hat{r})^2 \right]^{1/2}. \tag{3.31}$$

With this simplification, we finally have

$$B_\theta = \frac{\omega^2}{4\pi}\frac{e^{i\omega(r-t)}}{r}\left\{\left[\vec{p}_R^{\,2}-(\vec{p}_R\cdot\hat{r})^2\right]^{1/2}\cos\left[\left(k_0 r-\vec{k}\cdot\vec{r}\right)+\vartheta_R\right]\right.$$
$$\left.+\,i\left[\vec{p}_I^{\,2}-(\vec{p}_I\cdot\hat{r})^2\right]^{1/2}\cos\left[\left(k_0 r-\vec{k}\cdot\vec{r}\right)+\vartheta_I\right]\right\} \tag{3.32}$$

$$B_\phi = \frac{\omega^2}{4\pi}\frac{e^{i\omega(r-t)}}{r}\left\{\left[\vec{p}_R^{\,2}-(\vec{p}_R\cdot\hat{r})^2\right]^{1/2}\sin\left[\left(k_0 r-\vec{k}\cdot\vec{r}\right)+\vartheta_R\right]\right.$$
$$\left.+\,i\left[\vec{p}_I^{\,2}-(\vec{p}_I\cdot\hat{r})^2\right]^{1/2}\sin\left[\left(k_0 r-\vec{k}\cdot\vec{r}\right)+\vartheta_I\right]\right\}. \tag{3.33}$$

The phase ϑ_R was previously given, and the phase for the imaginary part ϑ_I may be determined analogously. Since these expressions separate the dipole moment $\vec{p}$ only into its real and imaginary parts, and not on the specific planar form (3.14), they must actually hold for arbitrary $\vec{p}$ (although with a more general $\vec{p}$ the specific formulas for the phases ϑ_R and ϑ_I would need modification).

From (3.32) and (3.33), it is evident that the radial component of the unmodified Poynting vector (3.28) is unaffected by k^μ even when the oscillating dipole is generating elliptically polarized radiation. This is actually not unexpected, for dimensional reasons. $\vec{S}$ has units of energy per unit area per unit time, or (momentum)^4. The field strengths $\vec{E}$ and $\vec{B}$ are each proportional to ω^2, so there is no way for a product of the E and B fields we have found to give a quantity with the right dimensions that also depends linearly on k^μ. However, there are still other terms through which the energy and momentum outflows might be modified.

3.4 Further Possibilities for Energy-Momentum Flow

These additional possibilities come in two types. One of them arises from the fact that, as already noted, $\vec{S}^{(0)}$ is not the correct expression for the energy flux density

or the momentum density. There are additional terms appearing in (3.4) and (3.5) involving the potentials A_0 and $\vec{A}$. Since the potentials are normally linearly proportional to ω, and because the novel terms [with the forms $\vec{\mathcal{P}}^{(1)} = -\vec{k}\left(\vec{A}\cdot\vec{B}\right)$ and $\vec{S}^{(1)} = -k_0 A_0 \vec{B} + k_0 \vec{A}\times\vec{E}$] also depend linearly on k^μ, we expect that they may give rise to dimensionally correct corrections to the energy and momentum flow that are proportional to $k\omega^3$.

The other way in which additional contributions to the energy and momentum transport might arise would be if the circular polarization vectors (3.9) were insufficiently accurate. When k^μ is purely timelike, the $\hat{\epsilon}_\pm$ are the exact polarization vectors for propagating plane wave modes. However, if $\vec{k} \neq 0$, these forms are only approximate, and the corrections can become substantial when k^μ is spacelike, for propagation along directions $\hat{r}$ for which $k^\mu \cdot \hat{r}_\mu = k_0 - \vec{k}\cdot\hat{r}$ is small. Possibly compensating for this, however, is the fact that these are exactly the directions for which the splitting in the dispersion relation (3.10) is also small.

One potentially tricky fact about the modified polarization states is that the basis vectors for the normal modes of propagation do not need to be same for the $\vec{E}$ and $\vec{B}$ fields. This is evident, for example, from the divergence equations for plane waves in vacuum. Gauss's law is modified,

$$i\vec{Q}\cdot\vec{E} = 2\vec{k}\cdot\vec{B}, \tag{3.34}$$

but $i\vec{Q}\cdot\vec{B} = 0$ is not. So the polarization basis vectors for $\vec{E}$, but not for $\vec{B}$, may acquire longitudinal components. Moreover, the other homogeneous Maxwell's equation (Faraday's law),

$$i\vec{Q}\times\vec{E} = i\omega\vec{B}, \tag{3.35}$$

still provides the relationship between the polarization bases for the two fields.

In fact, the exact polarization vectors for arbitrary k^μ are known. The transverse polarization vectors for the magnetic field are [85, 27, 74]

$$\hat{\epsilon}_\pm^{(B)} \propto \left(\omega^2 - Q_\pm^2\right)\hat{\theta} - 2i\left(k_0 Q_\pm - \omega\vec{k}\cdot\hat{r}\right)\hat{\phi}. \tag{3.36}$$

However, in order to find the k-linear corrections to these polarization vectors, it is necessary to use a more precise expression for the relationship between ω and $Q_\pm$. This is discussed in section 3.4.2.

3.4.1 Explicit Modifications to $\Theta^{\mu\nu}$

Note that, in general, these two types of pathways for finding contributions to the net energy and momentum outflow could potentially come into play simultaneously. Since the modified polarization vectors depend nonperturbatively on the components of k^μ, there is no straightforward power counting argument that the modified polarization structure cannot play a role in contributions from terms like $k_0\vec{A}\times\vec{E}$. However, there is a straightforward power counting argument that the modified polarization structure cannot, at leading order, play a role in physical contributions from $\vec{S}^{(1)}$ and $\vec{\mathcal{P}}^{(1)}$. When expanding all quantities in powers of k^μ and neglecting all modifications beyond linear order, the explicit presence of a k^μ component in a formula such as $k_0\vec{A}\times\vec{E}$ would mean that we would only need to use the conventional expressions for $\vec{A}$ and $\vec{E}$, as derived in the Lorentz-invariant Maxwell theory. In any case, from the fact that the propagating $\vec{B}$ remains exactly transverse even in the Chern-Simons theory, we can actually conclude that the $-k_0 A_0\vec{B}$ term can

never contribute to a net energy outflow away from the dipole, since the dot product of this term with $\hat{r}$ is vanishing.

Nonetheless, it is worth adding a few words about the peculiar character of the scalar potential in the kind of analysis that we are undertaking. The standard form for the (seemingly) propagating part of the scalar and vector potentials in the Lorenz gauge (which is frequently considered the most convenient for radiation problems) are

$$A_0 = -i\frac{\omega}{4\pi}\,(\hat{r}\cdot\vec{p})\,\frac{e^{i\omega(r-t)}}{r} \tag{3.37}$$

$$\vec{A} = -i\frac{\omega}{4\pi}\,\vec{p}\,\frac{e^{i\omega(r-t)}}{r}. \tag{3.38}$$

For $\vec{A}$, it appears to be straightforward to separate this expression into separate right- and left-circular polarization modes, which can each then be modified to account for the nonstandard energy-momentum relation in the Chern-Simons theory. However, this methodology does not appear to be applicable to A_0, precisely because it is a scalar quantity with no reference to polarization directions. Moreover, A_0 evidently only depends on the radial component of the $\vec{p}$, whereas in the standard theory the $\hat{r}\cdot\vec{p}$ component of the dipole moment is precisely the part which does not affect the $\vec{E}$ and $\vec{B}$ radiation fields in the direction $\hat{r}$. Clearly, an A_0 with this form cannot contribute to any physically observable characteristics of the emitted radiation; in fact, the role that A_0 actually plays is simply to cancel other equally unphysical contributions to $\vec{E}$ that come from the longitudinal component of $\vec{A}$. The reason that there is no straightforward separation of A_0 into two pieces, associated with the two physical polarization modes, is that A_0 is actually only associated with the

unphysical longitudinal mode—which, quite naturally, does not even really have a well-defined dispersion relation. Moreover, had we chosen a transverse gauge with $\vec{\nabla} \cdot \vec{A} = 0$, the far-field, wavelike part of A_0 would have been vanishing and the issue of trying to disentangle to right- and left-handed modes in the scalar field would never have arisen.

This, in turn, suggests another interesting possibility. We have already observed that the radial component of the first term in $\vec{S}^{(1)} = -k_0 A_0 \vec{B} + k_0 \vec{A} \times \vec{E}$ is necessarily zero, because of the structure of $\vec{B}$; this is true regardless of what form A_0 takes and thus whatever gauge conditions have been imposed. It is then tempting to wonder whether it might be possible, with a judicious choice of gauge, to make the radial component of the second term also vanish! However, we shall set this question aside for now, in favor of a direct evaluation of $\vec{A} \times \vec{E}$ in the Lorenz gauge.

The separation of $\vec{A}$ into its two circularly-polarized components follows straightforwardly along the same lines as the separation of the magnetic field $\vec{B}$. The analogue of (3.12) is

$$\vec{A} = -i \frac{\omega}{4\pi} \frac{e^{i\omega(r-t)}}{r} \sum_{\pm} \left(\hat{\epsilon}_{\pm}^{*} \cdot \vec{p} \right) e^{\pm i \left(k_0 r - \vec{k} \cdot \vec{r} \right)} \hat{\epsilon}_{\pm} + \vec{A}_L . \tag{3.39}$$

Although the two vectors $\hat{\epsilon}_{\pm}$ do not form a complete basis for three-dimensional space, they do span the two-dimensional space of transverse polarizations. The (longitudinal) remainder term $\vec{A}_L$ is unphysical, with its contributions to the electric field $\vec{E}$ being canceled by those coming from A_0. In the transverse gauge, $\vec{A}_L = 0$, and we shall adopt this simplifying convention henceforth. The full decomposition may be carried out, but it is simpler to notice that if $A_0 = 0$ (which is the case in the far field if $\vec{A}_L = 0$ also), then we simply have $\vec{A} = \vec{A}_T = -\frac{i}{\omega} \vec{E}$.

Consequently, the outward component of the explicit modified part of the formula for $\vec{S}$ is

$$\vec{S}^{(1)} \cdot \hat{r} = \frac{1}{2} k_0 \Re \left\{ -\frac{i}{\omega} \vec{E} \times \vec{E}^* \right\} \cdot \hat{r} = -\frac{k_0}{2\omega} \Re \left\{ i \left(E_\theta E_\phi^* - E_\phi E_\theta^* \right) \right\}. \tag{3.40}$$

If the dipole is oscillating linearly, so that $\vec{E}$ has a form of a real-valued vector field times a spherical wave phase factor $e^{i\omega(r-t)}$, then (3.40) is manifestly zero. However, for a complex dipole, (3.32) and (3.33) give

$$\vec{S}^{(1)} \cdot \hat{r} = \frac{k_0 \omega^3}{16\pi^2 r^2} \left[\vec{p}_R^{\,2} - (\vec{p}_R \cdot \hat{r})^2 \right]^{1/2} \left[\vec{p}_I^{\,2} - (\vec{p}_I \cdot \hat{r})^2 \right]^{1/2} \sin(\vartheta_R - \vartheta_I). \tag{3.41}$$

This looks like the signature of a new effect; however, this modification to the energy flow is actually illusory. Since $\vec{S}$ and $\mathcal{E}$ are not gauge invariant, the only physically meaningful measure of energy outflow is the total integral of $\vec{S} \cdot \hat{r}$ over the sphere at spatial infinity. While $\vec{S}^{(1)} \cdot \hat{r}$ may be nonzero in certain directions, it is odd as a function of angles, so that when integrated over the whole sphere, the result is necessarily vanishing. This can be seen from the previous expression for ϑ_R,

$$\vartheta_R = -\tan^{-1} \left[\frac{(p_1 \cos\phi + p_2 \cos\alpha \sin\phi) \cos\theta}{p_1 \sin\phi - p_2 \cos\alpha \cos\phi} \right], \tag{3.42}$$

and the similar formula for ϑ_I. Comparing the values of ϑ_R in antipodal directions (θ, ϕ) and $(\theta', \phi') = (\pi - \theta, \phi + \pi)$, the trigonometric functions $\cos\theta' = -\cos\theta$, $\cos\phi' = -\cos\phi$, and $\sin\phi' = -\sin\phi$ all change signs, so that $\vartheta_R' = -\vartheta_R$. Qualitatively, we might expect that the radial component of $\vec{S}$ should depend on the quantity $(\vec{p}_R \times \vec{p}_I) \cdot \hat{r}$, which is a pseudoscalar and so has opposite signs in the $\hat{r}$- and $(-\hat{r})$-directions. This is related to the fact that the net ellipticity, seen over the entire 4π range of solid angles, is expected to be zero, since any right-elliptically-polarized

waves emitted along $\hat{r}$ will be counterbalanced by left-elliptically-polarized emission in the antipodal direction.

For any modified contributions to the momentum outflow, it turns out that there is a very similar argument. Notice that in the explicitly k^μ-dependent term in (3.2), the second index is simply that of k^μ itself, so the spatial densities $\Theta^{0\nu}$ all have modifications of the form $-k^\nu \vec{A}\cdot\vec{B}$. The corresponding integrated quantities are the components of the electromagnetic energy-momentum four-vector,

$$P^\mu = -k^\mu \int d^3x\, \vec{A}\cdot\vec{B} = -k^\mu H, \tag{3.43}$$

proportional to the total magnetic helicity H [72, 66]. The relationships between the novel terms in the Poynting vector $\vec{S}$ and the Maxwell stress tensor is

$$\overleftrightarrow{T} \;=\; \overleftrightarrow{T}^{(0)} + \vec{k}\left(-A_0\vec{B} + \vec{A}\times\vec{E}\right) \;=\; \overleftrightarrow{T}^{(0)} + \frac{\vec{k}}{k_0}\vec{S}^{(1)}. \tag{3.44}$$

Since the net momentum loss rate of the radiation is the integral of $\overleftrightarrow{T}\cdot\hat{r}$ over the sphere at infinity, the vanishing of the integral of (3.40) over all directions dictates that the integral of analogous term for the momentum, $\overleftrightarrow{T}^{(1)}\cdot\hat{r}$ must also give zero.

3.4.2 Modified Polarization Structure

This leaves the only possible channel for modifications to the energy or momentum emission at $\mathcal{O}(k\omega^3)$ to be through the k^μ-modified polarization vectors (3.36). Along with (3.36) for $\vec{B}$, there are also the modified polarization vectors for the electric field [85, 27, 74],

$$\hat{\epsilon}^{(E)}_\pm \propto 2\left(k_0 Q_\pm - \omega\vec{k}\cdot\hat{r}\right)\hat{\theta} - i\left(\omega^2 - Q_\pm^2\right)\hat{\phi} + \left[\hat{\epsilon}^{(E)}_\pm\cdot\hat{r}\right]\hat{r}. \tag{3.45}$$

The radial term is nonzero, but its effects can be neglected. There are several reasons for this. Firstly, the radial component is smaller than the other two by a factor of $\mathcal{O}\left(k\omega^{-1}\right)$, so it only affects the normalization of $\hat{\epsilon}_{\pm}^{(E)}$ [noting that (3.36) and (3.45) are, as yet, not normalized] at linear order in k^{μ}. This radial term will also not affect the projection of the standard $\vec{E}$ (which is transverse, apart from nonpropagating terms that fall off rapidly with distance) onto $\hat{\epsilon}_{\pm}^{(E)}$. Finally, no radial $\vec{E}$ field can contribute to $\vec{S}^{(0)} \cdot \hat{r}$.

Therefore, to the order of interested, (3.35) still reduces to $\vec{E} = \vec{B} \times \hat{r}$, and so the expression (3.28) for the outgoing Poynting vector is still valid. However, the previous expressions for B_{θ} and B_{ϕ}—derived using (3.9) instead of (3.36)—are not. Instead, we must apply

$$\vec{B} = \frac{\omega^2}{4\pi} \frac{e^{i\omega(r-t)}}{r} \sum_{\pm} \left[\hat{\epsilon}_{\pm}^{(B)*} \cdot \left(\hat{r} \times \vec{p} \right) \right] e^{\pm i \left(k_0 r - \vec{k} \cdot \vec{r} \right)} \hat{\epsilon}_{\pm}^{(B)}. \tag{3.46}$$

Evaluating the components of $\hat{\epsilon}_{\pm}^{(B)}$ directly from (3.36) is actually trickier than it looks. Expanding the two components to leading order in k^{μ} and then normalizing, the k^{μ}-dependence actually cancels out, leaving just (3.9)! Instead, the most straightforward way to evaluate $\hat{\epsilon}_{\pm}^{(B)}$ is to notice that the $\hat{\theta}$- and $\hat{\phi}$-components of (3.36) also appear in the exact dispersion relation (3.11). Since the ratio of the components is known exactly, it immediately follows that

$$\hat{\epsilon}_{\pm}^{(B)} = \frac{1}{\sqrt{2}} \left[\left(1 - \frac{4 \left| \vec{k} \times \hat{r} \right|^2}{\omega^2 - Q_{\pm}^2} \right)^{-1/4} \hat{\theta} \pm i \left(1 - \frac{4 \left| \vec{k} \times \hat{r} \right|^2}{\omega^2 - Q_{\pm}^2} \right)^{1/4} \hat{\phi} \right] \tag{3.47}$$

$$= \frac{1}{\sqrt{2}} \left[\left(1 \mp \frac{1}{2} \frac{\left| \vec{k} \times \hat{r} \right|^2}{k_0 - \vec{k} \cdot \hat{r}} \right) \hat{\theta} \pm i \left(1 \pm \frac{1}{2} \frac{\left| \vec{k} \times \hat{r} \right|^2}{k_0 - \vec{k} \cdot \hat{r}} \right) \hat{\phi} \right]. \tag{3.48}$$

The approximation made in the last expression (3.48) is clearly dicey in the small ranges of angles for which $k^\mu \cdot \hat{r}_\mu$ is very small—$\mathcal{O}(k^2)$, instead of merely $\mathcal{O}(k)$. (And obviously, these angular ranges only exist for spacelike k^μ.) However, this should actually not pose a problem, because the birefringence itself vanishes as $k^\mu \cdot \hat{r}_\mu \to 0$. Note that the denominators in (3.47) are precisely $\omega^2 - Q^2$, so that when these quantities are $\mathcal{O}(k^2)$, the right-left difference in phase speeds is also $\mathcal{O}(k^2)$, meaning the propagation is conventional at leading order in k^μ.

The relative simplicity of the common factors in (3.48) means that the polarization vectors take the elliptical forms

$$\hat{\epsilon}_\pm^{(B)} = \hat{\epsilon}_\pm \mp \left(\frac{1}{2} \frac{\left| \vec{k} \times \hat{r} \right|^2}{k_0 - \vec{k} \cdot \hat{r}} \right) \hat{\epsilon}_\mp \equiv \hat{\epsilon}_\pm \mp \mathcal{T} \hat{\epsilon}_\mp. \tag{3.49}$$

With the angular dependence in (3.49), there does not appear to be any prospect for cancelations between the energy outflow in antipodal directions, since the term in parentheses (which we have denoted $\mathcal{T}$) does not simply change sign under $\vec{r} \to -\vec{r}$—unless, clearly, if $k_0 = 0$. In fact, if k^μ is spacelike, then there is an observer frame in which k_0 is indeed vanishing, and this is precisely the frame in which the stability of the theory is manifest, since the energy density $\mathcal{E} = \mathcal{E}^{(0)}$ is unmodified, meaning that the total energy is bounded below.

Moreover, since the $\mathcal{O}(k\omega^3)$ contributions to $\vec{S}$ that come from the k^μ-dependent terms in (3.49) come entirely from the $\vec{S}^{(0)}$ part of (3.4), these contributions are gauge invariant at the level of $\vec{S}$ itself, rather than only in integrated form. That suggests that it may be possible to identify the angular distribution of the emitted radiation, not merely the total rate of power emission. However, the gauge invariance of $\vec{S}^{(0)}$

does not, on its own, guarantee that it actually has a physical interpretation, since $\vec{S}^{(0)}$ is not actually the spatial part of a conserved energy-density current without the inclusion of the explicitly Lorentz-violating terms in $\Theta^{\mu\nu}$. From this directional information, in turn, it may be possible to find the net momentum being carried away, without having to perform any surface integrals of the stress tensor components.

The triple products needed for calculating $\vec{B}$ with the modified $\hat{\epsilon}_{\pm}^{(B)}$ polarization vectors are again given by (3.15). The calculation proceeds along the same lines as in section 3.3, and the result is the same—no change to the power emitted. However, there still remains the possibility that the radiation fields may carry away a net momentum, which can be calculated by integrating $\overset{\leftrightarrow}{T}{}^{(0)} \cdot \hat{r}$ over the sphere at spatial infinity. The dot product of the standard stress tensor $\overset{\leftrightarrow}{T}{}^{(0)}$ with the radial unit vector is

$$\overset{\leftrightarrow}{T}{}^{(0)} \cdot \hat{r} = \vec{E}\left(\vec{E} \cdot \hat{r}\right) + \vec{B}\left(\vec{B} \cdot \hat{r}\right) - \mathcal{E}^{(0)}\hat{r}. \tag{3.50}$$

Of the three terms on the right-hand side of (3.50), only the first can be associated with a $\mathcal{O}(\mathcal{T})$ net momentum outflow.

The explicit expression for the longitudinal part of the modified polarization vector (3.45) is fairly awkward. However, to leading order in k^{μ} and the far-field approximation, the radial component of the electric field may be found simply from the modified Gauss's law (3.6), which reduces to

$$i\omega E_r = 2\vec{k} \cdot \vec{B}. \tag{3.51}$$

Note that this means that the leading contribution to the radial field E_r simply depends linearly on k^{μ}, rather than via the more elaborate nonperturbative quantity

$\mathcal{T}$, and this actually presages the fact that this term too will have a vanishing net contribution to the total energy-momentum outflow. In fact, there is already a clear issue with the $\vec{E}E_r$ term in $\overleftrightarrow{T}^{(0)} \cdot \hat{r}$. Because of the vacuum birefringence, the direction of $\vec{E}$ corkscrews around, varying with distance. This r-dependent behavior means that $\overleftrightarrow{T}^{(0)} \cdot \hat{r}$ cannot have a gauge-independent interpretation, describing the emission of momentum in different directions in a fashion than can be verified experimentally. Evaluating $\overleftrightarrow{T}^{(0)} \cdot \hat{r}$ at different large r values along a single ray will give vector expressions pointing different directions. At this stage, however, this does not necessarily rule out having a well-defined, nonvanishing, k^μ-dependent modification to the total momentum outflow rate, found by integrating $\overleftrightarrow{T}^{(0)} \cdot \hat{r}$ over a sphere at large r, if the angular integration conspires to make the directional variability seen along different rays cancel out, producing an integrated quantity that does not have such an unphysical dependence on r.

However, this turns out not to happen, and instead the momentum outflow rate, $\overleftrightarrow{T}^{(0)} \cdot \hat{r}$ integrated over a sphere at $r \to \infty$, simply vanishes. This may be seen explicitly by decomposing the expression into Cartesian components—and the result is actually the most straightforward in the $\vec{k}$-direction, which is precisely the direction in which we would expect a net momentum transfer to be most likely. (This is the direction in which a stationary charge emits vacuum Cerenkov radiation, for example.) In this direction, the key contribution comes from

$$\begin{aligned}
\left(\vec{E}\cdot\vec{k}\right)\left(\vec{E}\cdot\hat{r}\right) &= \left[\left(\vec{B}\times\hat{r}\right)\cdot\vec{k}\right]\left(-\frac{2i}{\omega}\vec{B}\cdot\vec{k}\right) && (3.52)\\
&= -\frac{1}{\omega}\Re\left\{i[k_\theta^2 B_\phi B_\theta^* - k_\phi^2 B_\theta B_\phi^* && (3.53)\\
&\quad + k_\theta k_\phi\left(B_\phi B_\phi^* - B_\theta B_\theta^*\right)]\right\}. && (3.54)
\end{aligned}$$

The $k_\theta k_\phi$ term is purely imaginary and so vanishes when the real part is taken. On the other hand, the k_θ^2 and k_ϕ^2 terms vanish when integrated over all angles, just as happened with the expression in (3.40).

3.5 Conclusions and Outlook

The net result of our calculations is therefore that the Larmor power emission, which (along with vanishing net momentum outflow) characterizes the radiation from a classical oscillating dipole, is unchanged in the Lorentz-violating Chern-Simons theory at leading order in the size of the Lorentz violation coefficients. This is not actually extremely unexpected. Indeed, one might be tempted to argue that the vanishing results ought to follow from the discrete symmetries of the Chern-Simons term alone. The operator parameterized by k_0 is odd under parity, while those parameterized by $\vec{k}$ are odd under time reversal. However, this is probably too facile, since our calculations went beyond a perturbative power-series expansion in the components of k^μ. We considered the $k^\mu r_\mu \gg 1$ regime and thus effectively resummed certain terms to all orders in k^μ. This allowed for the inclusion of the key phenomenon of polarization rotation, which we found—in the discussion of $\overleftrightarrow{T}^{(0)}$—could actually lead to useful insights about the extent to which various quantities could be assigned gauge-independent physical interpretations. Equally interesting was the appearance of the fundamentally nonperturbative quantity $\mathcal{T}$ in the transverse components of the modified polarization vectors. [It is the case, however, that whenever a key quantity to be integrated over all angles can be expressed using a form like (3.51)—with the k^μ-dependent right-hand side taking the form of the first term in an uncomplicated-

looking power-series expansion—the axial vector character of k^μ does guarantee that the integral must vanish.]

The peculiar form of $\mathcal{T}$ offered a possible mechanism for how symmetry-driven angular cancellations could be evaded—although that mechanism did not actually come into action at the orders we were considering. All the energetic quantities that involved $\mathcal{T}$ specifically turned out to have their $\mathcal{T}$-dependent behavior cancel out along each individual emission direction; in spite of the nonperturbative modifications to the polarization structure, the Poynting vector maintained the standard form (3.28).

Nevertheless, the structure of $\mathcal{T}$ does provide some guidance for understanding how the radiation structure will be modified at higher orders in the Lorentz violation, and there is no question that there will be modifications at the next order in k^μ; this was already demonstrated with the calculation of the vacuum Cerenkov emission in the theory with a spacelike k^μ. For an oscillating dipole composed of point charges separated by a characteristic size $d \sim v/\omega$, the $\mathcal{O}(q^2k^2)$ factor in the Cerenkov emission rate for the individual moving charges is $\mathcal{O}(p^2k^2\omega^2)$—leaving out the Cerenkov radiation's dependence on the charge velocity v, which is complicated and fundamentally nonperturbative; even a stationary charge may spontaneously radiate unless $k_0 = 0$. Thus, the expected $\mathcal{O}(p^2k^2\omega^2)$ emission rate behavior found in the Cerenkov process agrees with what we would expect to find from extending the formalism in this paper to the next order in k^μ; and it may actually be interesting to connect the formalism we have used to the Cerenkov radiation calculations by carrying out that extension. Since radiation damping is fairly easily described in the

standard oscillating dipole system, such calculations could provide a way of finding a generalized radiative friction term applicable in the Lorentz-violating theory.

Moreover, all these questions about radiation are also naturally connected to questions about the behavior of photonic quanta in the Chern-Simons theory. The quantization of the theory would lead to further changes in how energy-momentum is transported to infinity, although we appear to be limited in our ability to quantize the Chern-Simons theory, due to the energy instability created by the time component of k^μ. The potential divergence of the energy density can be seen directly in the formula (3.3) for $\mathcal{E}$. The instability can also be seen by evaluating the group velocity of the negative-frequency modes [24]. To deal with this obstruction, it appears that we must bound the energy density from below, so that the quantum states of the theory can be built up in the usual way as excitations atop the vacuum. In fact, a spacelike CPT-odd axial vector k^μ picks out a preferred frame in which the energetics are well behaved; the theory may be quantized in the $k_0 = 0$ reference frame. The existence of this special frame, where the stability of the energy density is manifest from the form of $\mathcal{E}$, affects the structure of vacuum Cerenkov radiation in the spacelike theory. A charged particle moving with a velocity $\vec{v}$ which exceeds the phase speed of light will emit radiation, and the radiation applies a back-reaction force on the charge, which tends to bring the charge to rest in precisely the frame where k^μ has no temporal component. This connection between the condition for the energy to become stable and the dynamics of individual charges was a very important motivation for the current work. It seems that there should also be a connection between the radiative reaction force on a dipole that is emitting radiation by oscillating, but the order of

calculations in this paper has not been sufficient to capture this phenomenon.

Another obvious direction along which the calculations in this paper could be generalized would be to look at radiation from higher-ℓ multipoles. However, our expectation based on what we have found for the electric dipole case is that there would again be no leading-order k^μ-dependent effects. Nevertheless, it may be an interesting mathematical physics exercise to generalize the methods we have utilized in this paper to account for radiation in all possible electric and magnetic multipole modes.

Chapter 4

Title of manuscript:

Dalitz Plot Kinematics for a Lorentz-Violating Three-Body Decay

[1]

[1] J. O'Connor and B. Altschul, Submitted to Physical Review D, 26 June 2025

4.1 Outline

Well-developed discussions of certain scattering cross sections, decay rates, and radiation emission rates in the presence of Lorentz symmetry breaking, and kinematic considerations are often of uppermost importance. Many of the modifications to the standard theory that are necessary are described in Ref. [32]; as an example, the authors calculate the cross section for pair annihilation in the limit where particle momentum is greater than its mass but still far below the Planck energy. In Ref. [14], the Compton scattering cross section is computed in the presence of a Lorentz and CPT-breaking background that affects the electron. In that case, since the Lorentz violation breaks the spin degeneracy of the external state, the velocity and phase space factors in the kinematics depend on the particles' spins; therefore Casimir's trick for polarization sums does not work for calculating the unpolarized cross section—which means the modified kinematics cause a fundamental change in how the rate for the process has to be calculated. The cross section needs to be determined using a basis of explicit polarization states for all the incoming and outgoing particles, which can be quite complicated, even with a single isotropic but Lorentz-violating b_μ term added to the action. The scattering cross section differs greatly from the Klein-Nishina formula, and despite the complexity, the calculation can be performed non-perturbatively in b_μ, making it possible to observe that the cross section actually diverges at low photon energies—in sharp contrast to the predictions of various low-energy theorems that assume Lorentz invariance. Next, we summarize our second manuscript, which gives a systematic analysis in a similar fashion. In Ref. [48], we look for changes to the conventional classical electrodynamics

Larmor radiation expression in presence of Lorentz and CPT violating terms in the photon sector. In the electromagnetic sector of the minimal SME, there may exist a Chern-Simons-like Lorentz-violating term. In addition to being of intense theoretical interest because of its unusual gauge-symmetry properties and their relationship to radiative corrections, this term modifies the dispersion relations for electromagnetic waves (in a polarization-dependent fashion). This opens up the possibility of a Cerenkov-type effect in vacuum, which is discussed in [85], which calculates the exact radiation rate using the modified field equations and shows that they essentially agree with the phase-space estimate. The phase space estimate is calculated using a standard matrix element, combined with an evaluation of the available outgoing phase space for the single almost-circular polarization mode into which radiation is kinematically allowed. These kinematic considerations can also be extended to a broad class of SME coefficients in the charged fermion sector [13, 93].

Although research in modern particle theories emphasizes the calculation of matrix elements, in this chapter we show that under the SME, the kinematics of scattering and decay processes can be just as important as, and in many cases more important than, the matrix elements $i\mathcal{M}$. Thus, the quantum regime in the Standard Model will be extended through modified phase space. Extensions of our previous work [48] are found through examination of major aspects of Lorentz-violating quantum field theories with emphasis on the behaviors of the modified particle momenta and energies [21], and how they affect decay kinematics. We shall look specifically at three-body decay rates with Lorentz violation, performing computations with a modified outgoing phase space. Therefore, with a similar methodology, decay rates

are calculated in a simple model, with a parent particle such as a kaon or η meson decaying into three identical pions, in the presence of Lorentz-violating but CPT-preserving background tensor $c_{\mu\nu}$ which modify the kinematics for the daughters. In addition to outlining every step of the calculation for the decay rate, we shall look at how the Lorentz violation affects the boundaries of the allowed region of the Dalitz plot for the process.

This chapter is based on newly completed work that can be found in Ref [22], and is organized as follows. In section 4.2, we outline the specific type of SME theory that we shall be using in our kinematics calculations. In section 4.3, we consider two specific textures for the Lorentz-violating background tensor $c_{\mu\nu}$, outlining the practicalities of calculating a three-body decay rate with a modified space. Section 4.4 turns to the determination of the boundaries of the Dalitz plot for the decay process, delimitating the kinematically allowed region in the plane of the two independent mass-squared parameters. Finally, Section 4.5 summarizes our conclusion and discusses the possible areas for future investigation.

4.2 Lorentz-Violating Field Theory

Research in modern particle theories emphasizes the calculation of transition matrix elements, meaning the dynamics. However, the kinematics of scattering and decay processes can be just as important or in many cases more important than the matrix elements $i\mathcal{M}$. The reason for this is that the kinematical and the dynamical parts of a differential rate calculation can be separated out rather neatly. For a constant matrix element, even in the fully integrated rate the effects of kinematics and dynamics can

be calculated as independent multiplicative factors, although more generally the two are mixed in the integration over all channels. Since the kinematic factors depend only on the behavior of the free asymptotic incoming and outgoing particles, they do not need to be calculated anew for each process—at least in a conventional theory with standard energy-momentum relations for all the particle species.

Phase space modifications due to Lorentz violation can increase the number of singularities in the integrand and the boundary conditions in any integral for the decay rate Γ, and the calculational approaches for specific decay processes must be transformed in such ways as to address these added complications. With anisotropic Lorentz-violating terms in the Lagrange density for each outgoing particle, the angular integration may make calculating Γ highly nontrivial, since when we include such terms the particle energies depend on the angular orientations of the outgoing particles' motions. Therefore, before exploring more elaborate modified decay integrals in the future, we shall consider in this paper a particularly simple model. The parent particle will decay into three daughters with equal mass, vanishing spin, and identical Lorentz violation parameters.

The dispersion relation for the π field—from which all the kinematic information may be derived—has the relatively simple Lorentz-violating form

$$(g^{\mu\nu} + 2c^{\mu\nu})\, p_\mu p_\nu - m^2 = 0. \tag{4.1}$$

The notation $k_{\mu\nu}$ for $2c_{\mu\nu}$ is often used in the context of spinless fields, with $c_{\mu\nu}$ restricted to the physically analogous coefficients for fermions. However, since our analysis here will focus purely on kinematics, the results should be equally valid for out-

going scalars and spinors, provided the Lorentz violation is of the spin-independent $c_{\mu\nu}$ type. We therefore opt to use the notation with $c_{\mu\nu}$ even for bosonic fields.

To canonically quantize a theory with $c_{\mu\nu}$-type Lorentz violation—whether the scalar theory in (2.5) or its fermionic analogue—it is generally useful to rescale the field and the mass parameter m. In the Klein-Gordon theory, that means a rescaling so that the Lagrange density does not contain nonstandard double time derivatives $c_{00}\partial^0\partial^0$. This may always be accomplished, because we may always subtract a term proportional to $g_{\mu\nu}$ from $c_{\mu\nu}$, transferring the double time derivative from the SME term to the conventional Klein-Gordon kinetic term in (2.5). Following this transformation and a rescaling of π and m, the Lagrange density still has the general form (2.5), albeit with different values for the diagonal components of the background tensor. This rescaling, because it changes the normalization of the quantized field, will appear in the matrix elements for any processes involving the π field. However, as we shall not be concerned here with the details of matrix element calculations—basing our results purely on the kinematical corrections derived from the modified dispersion relation (4.1)—we will not need to delve into that issue in detail.

4.3 Decay Phase Space

We begin with a general description of the differential decay rate for a channel with three identical spinless particles in the final state; for definiteness, we shall take these daughter particles to be pions. Beginning with a fairly general description, we shall make successive simplifying assumptions in order to make calculations reasonably tractable. To start with, the differential decay rate for a channel in which the three

outgoing pion four-momenta are p, k, and l is

$$d\Gamma = \frac{(2\pi)^4}{2}\frac{|\mathcal{M}|^2}{\sqrt{s}}\, d^4p\, d^4k\, d^4l\, \delta(\xi_p)\, \delta(\xi_k)\, \delta(\xi_l)\, \delta^4(P-p-k-l). \tag{4.2}$$

This will form the integrand of the modified decay integral, with modified quadratic Lorentz-violating dispersion relations visible in the first three Dirac δ-functions. These enforce the energy-momentum relations for each of the three pions in the final state. If the initial unstable particle is at rest, so that $P^\mu = (\sqrt{s}, \vec{0}\,)$, the three daughter three-momenta line in a plane. We may therefore take the spatial momentum of the first daughter pion to define the $-z$-direction, $p^\mu = (E_p, 0, 0, -|\vec{p}\,|)$, with the other two daughter trajectories also lying in the xz-plane. In the rest frame of the parent particle, θ is the angle between $\vec{p}$ and $\vec{k}$, and α is the angle between $\vec{l}$ and $\hat{z}$. This configuration is show in figure 4.1. (Note that because of the anisotropy in $c_{\mu\nu}$, the three-momentum of a particle may point in a slightly different direction from its velocity.)

Furthermore, we shall eventually assume that $\sqrt{s} \gg m$, so that the outgoing mesons are ultrarelativistic. For the fermionic theory with $c_{\mu\nu}$, which has a slightly more intricate structure than the scalar theory, the ultrarelativistic limit results in some additional simplifications. For the scalar theory, or for the ultrarelativistic

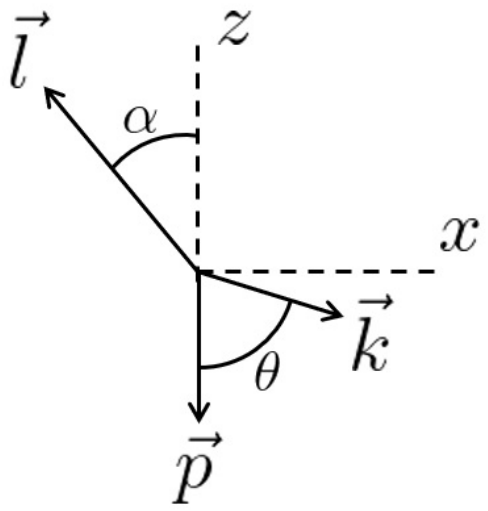

Figure 4.1 Configuration of the x- and z-axes and the outgoing three-momenta in the plane of the decay.

Dirac theory, the arguments of the first three δ-functions in the expression for $d\Gamma$ are

$$\xi_p = (1+c_{00})\,E_p^2 - c_{03}\,|\vec{p}|\,E_p - (1+c_{33})\,|\vec{p}|^2 - m^2 \tag{4.3}$$

$$\begin{aligned}\xi_k &= (1+c_{00})E_k^2 + (c_{01}\sin\theta - c_{03}\cos\theta)|\vec{k}|E_k \\ &\quad -(1-c_{11}\sin^2\theta - c_{33}\cos^2\theta + c_{13}\sin\theta\cos\theta)|\vec{k}|^2 - m^2\end{aligned} \tag{4.4}$$

$$\begin{aligned}\xi_l &= (1+c_{00})E_l^2 + (c_{01}\sin\alpha + c_{03}\cos\alpha)|\vec{l}\,|E_l \\ &\quad -(1-c_{11}\sin^2\alpha - c_{33}\cos^2\alpha + c_{13}\sin\alpha\cos\alpha)|\vec{l}\,|^2 - m^2.\end{aligned} \tag{4.5}$$

The angular structure that arises from integration over all allowed momenta is extremely complicated if the texture of $c_{\mu\nu}$ is allowed to contain all nine physically distinguishable parameters, describing generic forms of rotation and boost invariance violations in the pion kinetic energy. So a simplifying assumption is desirable,

as our principal goal is to describe the complications that arise in evaluations of the three-body decay phase space factor in the context of the SME. In the literature, as a way of reducing a general symmetry violation problem to one with just a single parameter describing the extent of the Lorentz violation, it is common to consider a theory that is isotropic (in the lab frame or some other natural frame, such as the rest from of the cosmic microwave background; in that particular frame, only the Lorentz boost symmetry is broken).

However, in a case like this one, the isotropic theory is actually too simple. With identical ultrarelativistic daughter particles, the Lorentz-violating modifications in an isotropic theory can be reduced to a simple rescaling of the conventional result. Actually, this is a fairly natural conclusion. The complexity of the $d\Gamma$ in (4.2) comes from the angular structure, and if there is no anisotropy $c_{0j} = 0$ and c_{jk} is proportional to δ_{jk}, which wipes out all the angular structure in (4.3–4.5). If there are no angular dependences, it does not meaningfully matter which directions the daughter pions are moving; all the changes is an overall rescaling of the dependence of the particle energy on the spatial momentum. So we shall instead introduce a different simplifying parameterization of the background tensor $c_{\mu\nu}$.

4.3.1 Single-Coefficient Model

Analogous to an isotropic limit, we could set all the c coefficients equivalent, $c_{\mu\nu} = c\mathbf{M}_{4\times4}$, where all the components of the matrix $\mathbf{M}_{4\times4}$ are equal to 1. A theory with a $c_{\mu\nu}$ background tensor of this form is certainly not Lorentz invariant; only if $c_{\mu\nu} \propto g_{\mu\nu}$ is the Lorentz symmetry unbroken. However, it can be slightly trickier to identify

whether or not a SME-type theory is isotropic in some particular preferred frame. In this case, $c_{\mu\nu} = c\mathbf{M}_{4\times4}$ is not an isotropic texture, as there is a clearly preferred direction, $(\hat{x}+\hat{y}+\hat{z})/\sqrt{3}$. So nontrivial anisotropy is preserved, while still making the modifications to the conventional theory depend on just a single dimensionless parameter c. The differential decay rate with this type of $c_{\mu\nu}$ is

$$\begin{aligned} d\Gamma &= \frac{(2\pi)^4}{2}\frac{|\mathcal{M}|^2}{\sqrt{s}}\, d^4p\, d^4k\, d^4l\, \delta[(1+c)E_p^2 - c|\vec{p}\,|E_p - (1+c)\,|\vec{p}\,|^2 - m^2] \\ &\quad \times \delta\left[(1+c)E_k^2 + c(\sin\theta - \cos\theta)|\vec{k}|E_k - (1-c+c\sin\theta\cos\theta)|\vec{k}|^2 - m^2\right] \\ &\quad \times \delta\left[(1+c)E_l^2 + c(\sin\alpha + \cos\alpha)|\vec{l}\,|E_l - (1-c+c\sin\alpha\cos\alpha)|\vec{l}\,|^2 - m^2\right] \\ &\quad \times \delta^4(P-p-k-l). \end{aligned} \tag{4.6}$$

However, it is possible to simplify this expression even somewhat further while still retaining nontrivial angular anisotropy. The calculation steps and final expression are simplified greatly if we set $c_{13} = c_{31} = 0$. A great deal more in-depth analysis of the physical process will be needed if the mixing of the x- and z-components is to be kept in our calculation. The angular analysis should be made quite complex if this extra dependence is to be considered, so the decay with this term non-zero will be evaluated later. For now we drop this term because without it a simple cancellation arises without angular approximations. This is, we set $c_{\mu\nu} = c\mathbf{M}'_{4\times4}$, where $\mathbf{M}'_{4\times4}$ agrees with $\mathbf{M}_{4\times4}$, except that $\left(\mathbf{M}'_{4\times4}\right)_{13} = \left(\mathbf{M}'_{4\times4}\right)_{31} = 0$. With this modification, the differential decay rate for the channel is

$$\begin{aligned} d\Gamma &= \frac{(2\pi)^4}{2}\frac{|\mathcal{M}|^2}{\sqrt{s}}\, d^4p\, d^4k\, d^4l\, \delta[(1+c)E_p^2 - c|\vec{p}\,|E_p - (1+c)\,|\vec{p}\,|^2 - m^2] \\ &\quad \times \delta\left[(1+c)E_k^2 + c(\sin\theta - \cos\theta)|\vec{k}|E_k - (1-c)|\vec{k}|^2 - m^2\right] \\ &\quad \times \delta\left[(1+c)E_l^2 + c(\sin\alpha + \cos\alpha)|\vec{l}\,|E_l - (1-c)|\vec{l}\,|^2 - m^2\right]\, \delta^4(P-p-k-l). \end{aligned} \tag{4.7}$$

Continuing with the purely kinematical calculation, we may integrate over the momenta of the third particle. The δ-function that enforces overall momentum conservation sets $\vec{l} = -(\vec{p} + \vec{k})$, leaving

$$\begin{aligned} d\Gamma &= \frac{(2\pi)}{2} \frac{|\mathcal{M}|^2}{\sqrt{s}}\, d^4p\, d^4k\, dE_l \sum_{\pm} \\ &\quad \times \frac{\delta(E_l - \omega_l^{\pm})}{2|\omega_l^{\pm}|} \delta\Big[(1+c)E_p^2 - c|\vec{p}|E_p - (1+c)|\vec{p}|^2 - m^2\Big] \\ &\quad \times \delta\left[(1+c)E_k^2 + c(\sin\theta - \cos\theta)|\vec{k}|E_k - (1-c)|\vec{k}|^2 - m^2\right] \\ &\quad \times \delta\left[\sqrt{s} - E_p - E_k - E_l(\vec{l} = -\vec{p} - \vec{k}\,)\right]. \end{aligned} \tag{4.8}$$

Here, $\sum_{\pm} \delta(E_l - \omega_3^{\pm})$ appears because of the mathematical possibility of E_l, which is determined by a quadratic energy-momentum relation, could potentially takes roots $\omega_l^{\pm}(\vec{l})$ of either positive or negative sign. Physically, however, obviously only the positive-energy root

$$2\omega^+_{l=-p-k} = \sqrt{4(1+c)\left[(1-c)|\vec{p}+\vec{k}|^2 + m^2\right] + c^2\left[|\vec{p}| - |\vec{k}|(\sin\theta - \cos\theta)\right]^2} \tag{4.9}$$

contributes to the the decay rate.

Conversion of the energy-preserving δ-functions for the other two particles and dropping all but the positive, physical branches of the dispersion relations gives two more energy square root terms in the denominator

$$\begin{aligned} d\Gamma = \frac{1}{2(2\pi)^5} \frac{|\mathcal{M}|^2}{\sqrt{s}} &\frac{d^3p\, d^3k}{\sqrt{4(1+c)\left[(1-c)|\vec{p}+\vec{k}|^2 + m^2\right] + c^2\left[|\vec{p}| - |\vec{k}|(\sin\theta - \cos\theta)\right]^2}} \\ \times &\frac{\delta\left[\sqrt{s} - E_p - E_k - E_l\left(\vec{l} = -\vec{p} - \vec{k}\right)\right]}{\sqrt{|\vec{p}|^2(4-3c^2) + 4(1+c)m^2}\sqrt{|\vec{k}|^2(4 - 3c^2 - 2c^2\cos\theta\sin\theta) + 4(1+c)m^2}}. \end{aligned} \tag{4.10}$$

Since one of our principal focuses will be understanding the nature of any anisotropic effects due to the Lorentz violation, we could make a further approximation at this

point. Without the inclusion of $\mathcal{O}(c^2)$ terms in $d\Gamma$, there is no nonstandard angular dependence. However, since terms at this order are doubly small, it is of less profit to maintain them in our expressions when they are not specifically anisotropic. We could therefore drop terms of $\mathcal{O}(c^2)$ that do not also depend on θ; this entails, for example, the approximation $4 - 3c^2 \approx 4$. With this done, the approximate energies that appear in (4.10) would become

$$(1+c)E_p \approx \sqrt{|\vec{p}|^2 + (1+c)m^2} \tag{4.11}$$

$$(1+c)E_k \approx \sqrt{|\vec{k}|^2 + (1+c)m^2 - \frac{c^2}{2}|\vec{k}|^2 \sin\theta\cos\theta} \tag{4.12}$$

$$(1+c)E_l \approx \sqrt{\begin{array}{l} |\vec{p}+\vec{k}|^2 + (1+c)m^2 \\ -\frac{c^2}{2}\left[|\vec{p}||\vec{k}|(\sin\theta - \cos\theta) - |\vec{k}|^2 \sin\theta\cos\theta\right] \end{array}}. \tag{4.13}$$

However, we shall, for now, continue without this explicit simplification.

The next major step in the calculation is to deal with the energy conservation δ-function, which depends on the angles. This remaining δ-function in $d\Gamma$ has the complicated argument $\Delta = \sqrt{s} - E_p - E_k - E_l$, with the overall form,

$$\begin{aligned} \delta(\Delta) = \delta\Bigg(\sqrt{s} - \frac{1}{2(1+c)}\Bigg\{ & \sqrt{|\vec{p}|^2(4-3c^2) + 4(1+c)m^2} \\ & + \sqrt{|\vec{k}|^2(4 - 3c^2 - 2c^2\cos\theta\sin\theta) + 4(1+c)m^2} \\ & + \sqrt{\begin{array}{l} 4(1-c^2)|\vec{p}+\vec{k}|^2 + 4(1+c)m^2 + c^2[|\vec{p}| \\ -|\vec{k}|(\sin\theta - \cos\theta)]^2 \end{array}} \Bigg\}\Bigg). \end{aligned} \tag{4.14}$$

Implementation of this δ-function will entail multiplication by $|\partial\Delta/\partial\theta|^{-1}$. Ex-

plicitly, this angular derivative is

$$\left|\frac{\partial\Delta}{\partial\theta}\right| = \frac{1}{2(1+c)}\left\{\frac{4|\vec{p}||\vec{k}|\sin\theta}{E_l} + c^2\left[\frac{|\vec{k}|^2\cos 2\theta + |\vec{p}||\vec{k}|(\cos\theta - 3\sin\theta)}{E_l} + \frac{|\vec{k}|^2\cos 2\theta}{E_k}\right]\right\}. \quad (4.15)$$

Note that since the Lorentz-invariant term is always positive, the signs of the small Lorentz-violating corrections are unimportant to the determination of the absolute value.

After dividing the integrand in $d\Gamma$ by $|\partial\Delta/\partial\theta|$, the resulting integral is manageable at first order in c. The terms which depend on θ cancel after the term is divided into the integral and then the whole integrand approximated to first order in c. This avoids the complicated integration that would be necessary if the angular roots needed to be plugged back into the θ-dependent terms remaining in the integrand.

At this point, it is not possible to go further using only facts about the outgoing particle kinematics. For a generic process, the matrix element $i\mathcal{M}$ will also be a function of $\vec{p}$ and $\vec{k}$ (as well as the constrained momentum $\vec{l}$. The dependence can be both on the magnitudes of the three outgoing pion momenta and the angles between them. For the purpose of continuing our kinematical analysis, we must therefore make choice of what matrix element to use. To simplify things to the greatest extent possible—so as to keep the focus on what effects may be attributed purely to daughter particle kinematics—we shall opt for the simplest possible choice: a constant $|\mathcal{M}|^2$, such as might arise from a four-meson contant interaction of the form $\mathcal{L}_I \propto \lambda(\eta\pi^3)$. Henceforth, the $|\mathcal{M}|^2$ appearing in our expressions will be treated as a momentum-independent constant. This constant may generically include additional factors of c;

in particular, the rescaling of the π field to remove $c_{00}\partial^0\partial^0$ terms mentioned above can introduce $\mathcal{O}(c)$ momentum-independent corrections to the matrix element.

Although the approximation of constant $|\mathcal{M}|^2$ may seem rather drastic, it is not necessarily that unrealistic. The leading-order strong interaction matrix element for $\eta \to 3\pi^0$ in chiral perturbation theory is actually a momentum-independent constant [25] (although because the process violates isospin, the electromagnetic contribution to the matrix element is of similar size).

With the angular dependence of the matrix element squared known (and in our toy model case, trivial), it is possible to perform the angular integrations explicitly, at least to leading order in the Lorentz violation. The integration over the angular variables that the integrand does not depend upon (meaning over the direction of $\vec{p}$, and the azimuthal angle of $\vec{k}$ produces a factor a factor of $2(2\pi)^2$. The last angular integration over θ gives new factors that yield

$$\begin{aligned} d\Gamma &= \frac{1}{64\pi^2}\frac{|\mathcal{M}|^2}{\sqrt{s}}\, d|\vec{p}|d|\vec{k}| \\ &\times \frac{|\vec{p}||\vec{k}|(m^4 + m^2\left[|\vec{p}|^2(1+\frac{c}{2}) + |\vec{k}|^2(1+\frac{c}{2})\right] + |\vec{p}|^2|\vec{k}|^2(1+c))}{(|\vec{k}|^2+m^2)^{3/2}(|\vec{p}|^2+m^2)^{3/2}}. \end{aligned} \tag{4.16}$$

To simplify the remaining integration further, we can convert the integral in momentum to an integral over the unmodified on-shell energies

$$p^{(0)} = \sqrt{|\vec{p}|^2+m^2} \tag{4.17}$$

$$k^{(0)} = \sqrt{|\vec{k}|^2+m^2}. \tag{4.18}$$

The integral in terms of these conventional energies simplifies to

$$d\Gamma = \frac{1}{64\pi^2}\frac{|\mathcal{M}|^2}{\sqrt{s}}\, dp^{(0)}\, dk^{(0)} \left\{1 + c - \frac{c}{2}\left[\frac{m^2}{(p^{(0)})^2} + \frac{m^2}{(k^{(0)})^2}\right]\right\}. \tag{4.19}$$

Although we have not yet integrated over the magnitudes of the spatial momenta [or, equivalently, over $p^{(0)}$ and $k^{(0)}$], but only the associated angles, any momentum-dependent matrix element $i\mathcal{M}$ would need to by symmetric in $\vec{p}$, $\vec{k}$, and $\vec{l} = -\vec{p} - \vec{k}$; and the symmetric dependence on $\vec{l}$ means that if $i\mathcal{M}$ depends on the magnitudes of the three-momenta, it will also unavoidably depend on θ. So only with a completely constant matrix element may we reach this and later expressions.

We shall now impose the ultrarelativistic limit mentioned earlier. This allows us to neglect the mass scale m, except when it is needed to regulate logarithmic divergences in the infrared. With the $m \approx 0$ approximation, the first momentum integration is

$$d\Gamma = \frac{1}{64\pi^2} \frac{|\mathcal{M}|^2}{\sqrt{s}}\, dp^{(0)} \int\limits_{\frac{\sqrt{s}(1+c)}{2} - p^{(0)}}^{\frac{\sqrt{s}(1+c)}{2}} dk^{(0)} \left\{ 1 + c - \frac{c}{2} \left[\frac{m^2}{(p^{(0)})^2} + \frac{m^2}{(k^{(0)})^2} \right] \right\}. \tag{4.20}$$

We cannot use 0 as the lower bound in the subsequent p^0 integration, because of an infrared $\log(0)$ divergence. Instead, the lower bound must be cut off by the physical minimal value of $p^{(0)}$, which is m. This leaves, after integration over the $k^{(0)}$ energy,

$$\Gamma = \frac{1}{64\pi^2} \frac{|\mathcal{M}|^2}{\sqrt{s}} \int\limits_{m}^{\frac{\sqrt{s}(1+c)}{2}} dp^{(0)} \left[p^{(0)} + c \left(p^{(0)} - \frac{m^2}{2p^{(0)}} - \frac{2p^{(0)} m^2}{s - 2\sqrt{s} p^{(0)}} \right) \right]. \tag{4.21}$$

The calculation results in the ultimate decay rate

$$\Gamma = \frac{|\mathcal{M}|^2}{512\pi^2\sqrt{s}} \left[s(1+3c) - 4m^2 + 4cm^2 \log\left(\frac{2cm}{\sqrt{s} - 2m} \right) \right]. \tag{4.22}$$

The form of the c dependence in (4.22) is instructive. Note that although we expanded various expressions to $\mathcal{O}(c)$, the final expression's dependence on c is slightly different, containing a term of size $\mathcal{O}(c \log c)$. Naively, this looks like a slightly

stronger dependence on the coefficient c. However, the $\mathcal{O}(c\log c)$ term is also proportional to another small quantity, m^2/s.

4.3.2 Model with Nonzero c_{13}

If instead we keep all terms in $c\mathbf{M}_{4\times4}$, including the c_{13} term, things grow substantially more complicated, and angular approximations will be needed to get tractable analytical expressions. To ease the number of terms in the integrand for the decay rate, we will eventually use a series approximation that can be performed in θ to compute the angular part of the integral.

With the added angular dependence in the square root terms from the modified dispersion relations, the analog of (4.16), before θ-integration but with keeping the additional anisotropy term, is

$$\begin{aligned} d\Gamma &= \frac{1}{128\pi^3}\frac{|\mathcal{M}|^2}{\sqrt{s}}\,d|\vec{p}\,|d|\vec{k}|\,d\theta\,\frac{|\vec{k}|\csc\theta}{|\vec{p}\,|(|\vec{k}|^2+m^2)^{3/2}(|\vec{p}\,|^2+m^2)^{3/2}} \\ &\quad\times\Bigg(4|\vec{p}\,|^2\left\{(2+c)|\vec{p}\,|^2m^2+2m^4+|\vec{k}|^2\left[2(1+c)|\vec{p}\,|^2+(2+c)m^2\right]\sin\theta\right\} \\ &\quad+c(5|\vec{k}|^2+4m^2)(|\vec{p}\,|^2+m^2)|\vec{p}\,|^2\cos\theta+4c|\vec{k}||\vec{p}\,|(|\vec{p}\,|^2+m^2) \\ &\quad\times\left[|\vec{k}|^2+m^2-\sqrt{|\vec{k}|^2+m^2}\sqrt{|\vec{k}|^2+|\vec{p}\,|^2+m^2+2|\vec{p}\,||\vec{k}|\cos\theta}\right]\cos2\theta \\ &\quad+c|\vec{p}\,|^2|\vec{k}|^2\left[|\vec{p}\,|^2+m^2\right]\cos3\theta\Bigg). \end{aligned} \tag{4.23}$$

Because of the $\csc\theta$, the c-dependent part of the the above integral clearly diverges when the three daughter pions particles are colinear. This appears to be indicative of the previously noted fact that there may be a nonperturbative dependence on c where logarithms arise in the decay rate Γ; the $\mathcal{O}(c)$ approximations that we have made are inadequate near the poles at $\theta=0$ and π, where $\cos n\theta=(-1)^n$.

We could now regulate the integral equation by analytical continuation and use regulation techniques like asymptotic approximation [1], to account for the unusual Lorentz-violating behavior of the θ integration boundaries. However, if we merely continue the calculation by taking the indefinite integral over θ and using the fact that the θ integration region is symmetric around $\theta = \frac{\pi}{2}$, we note that the functions $\cos\theta$ and $\cos 3\theta$ are odd in $\vartheta = \theta - \frac{\pi}{2}$. Therefore, with the θ-independent matrix element squared $|\mathcal{M}|^2$, the terms with $\cos\theta$ and $\cos 3\theta$ will not make any $\mathcal{O}(c)$ contributions to the fully integrated Γ.

If the matrix element happened to be strongly peaked around $\vartheta = 0$, we might then further approximate, to first order in ϑ, that $\cos 2\theta = -1$. However, this is not a good approximation in the identical particle model we are using here. On the other hand, without the approximation, the angular integration becomes unavoidably tangled up with the integrals over $|\vec{p}|$ and $|\vec{k}|$. Going further and including the c-dependences of the limits of these latter integrations produces expressions too complicated to provide analytical insights, except insofar as we can see that it shares a somewhat similar logarithm structure to what we previously found in (4.22). If the expansion is made around $\theta = \frac{\pi}{2}$, the decay rate is,

$$\begin{aligned}\Gamma &= \frac{|\mathcal{M}|^2}{512\pi^2\sqrt{s}} \cdot \Big(\frac{s}{4} + m^2 - m\sqrt{s} + 4cs^{3/2} \cdot \big(4 + 8\sqrt{2} + (-6+\sqrt{2})\log\left(-1+\sqrt{2}\right) \\ &\quad - \left(-2+\sqrt{2}\right)\log\left(1+\sqrt{2}\right)\big)\Big) \end{aligned} \tag{4.24}$$

If the expansion is made around $\theta = \frac{\pi}{4}$, the form of Gamma gives another interesting expression for the decay rate, it is then

$$\Gamma = \frac{|\mathcal{M}|^2}{512\pi^2\sqrt{s}} \cdot (\sqrt{\frac{s-4m^2}{s-3m^2}} \cdot (4s - 12m^2) + 4m^2 \log(\frac{\sqrt{s-3m^2} - \sqrt{s-4m^2}}{m}) + \\ + c \cdot (\sqrt{\frac{s-4m^2}{s-3m^2}} \cdot (7m^2 - 3s))) + 4m^2 \log(\frac{\sqrt{s-3m^2} - \sqrt{s-4m^2}}{m})). \quad (4.25)$$

To complete the integration without any angular approximations, we need to find the poles in the boundary equation; we may do this by using (4.28) below. After insertion of the angle into (4.23), even when approximating to $\mathcal{O}(c)$ the integral is extremely long. If the approximation is further made of working only to first or second order in the mass m, the integral over the daughter momenta becomes more tractable; however, combined with the $\mathcal{O}(c)$ approximation (even with using the modified upper and lower bounds for the integration) the first-order dependence on m vanishes. Thus, to obtain a non-vanishing modification to the decay rate, the integral over on-shell daughter particle energies must be computed to at least $\mathcal{O}(m^2)$. The integration over one daughter energy yields a hugely complicated expression but with no explicit Lorentz violation terms remaining at leading order. However, after integration over the second on-shell energy, there is a c dependence, and the full decay rate at this order is

$$\Gamma = \frac{|\mathcal{M}|^2}{512\pi^2\sqrt{s}} \left[s(1+2c) + 4cm^2 + 4cm^2 \log\left(\frac{2mc}{\sqrt{s}-2m}\right)\right]. \quad (4.26)$$

4.4 Modified Dalitz Plots

For a three-body decay, studied in the center of mass frame, it makes sense to express the kinematics using a Dalitz plot. When all three outgoing particles are identical, with or without Lorentz violation, the Dalitz plot is symmetric with respect to the two

coordinate axes, since forming the scalar quantities m_{13}^2 and m_{23}^2 drops the leading order directional information. However, with non-identical daughters, the convex outline may take a more asymmetrical shape. At higher energies, as all particles become strongly relativistic, the shape approaches triangularity.

The interior of the allowed region of the plot is populated with a histogram of decay rates for different values of the parameters. The difference between a flat, uniform histogram and what is actually observed reveals the character of the dynamical matrix element. Dalitz plots are especially useful for displaying or recognizing information about final state interactions. If the invariant mass squared for two outgoing particles corresponds to a possible resonance intermediate, then there will be a line of resonance enhancement crossing the plot, something that can be easy to recognize in a plot of experimental data.

So we shall now explicitly calculate the modified boundary of the kinematically allowed region that arises from the inclusion of the Lorentz violation coefficients. This boundary condition arises from integration over the energy conservation δ-function; with a first order approximation in c and using the $c_{13} = 0$ model from section 4.3.1, the boundary condition is

$$\begin{aligned} \sqrt{s}(1+c) \;&-\; \left(\sqrt{|\vec{p}|^2+m^2}+\sqrt{|\vec{k}|^2+m^2}\right) - \frac{c}{2}\left(\frac{m^2}{\sqrt{|\vec{k}|^2+m^2}}+\frac{m^2+2|\vec{p}|^2}{\sqrt{|\vec{p}|^2+m^2}}\right) \\ &\leqslant\; \sqrt{|\vec{k}|^2+|\vec{p}|^2+m^2 \mp 2|\vec{p}||\vec{k}|} + \frac{cm^2}{2\sqrt{|\vec{k}|^2+|\vec{p}|^2+m^2\mp 2|\vec{p}||\vec{k}|}}. \end{aligned} \tag{4.27}$$

If c_{13} is not neglected, the expression (4.27) will remain unchanged; the presence of c_{13} only brings in terms which involve $\sin\theta$, and on the kinematic boundaries these terms vanish. Since the Lorentz violation coefficients c are small and three-pion

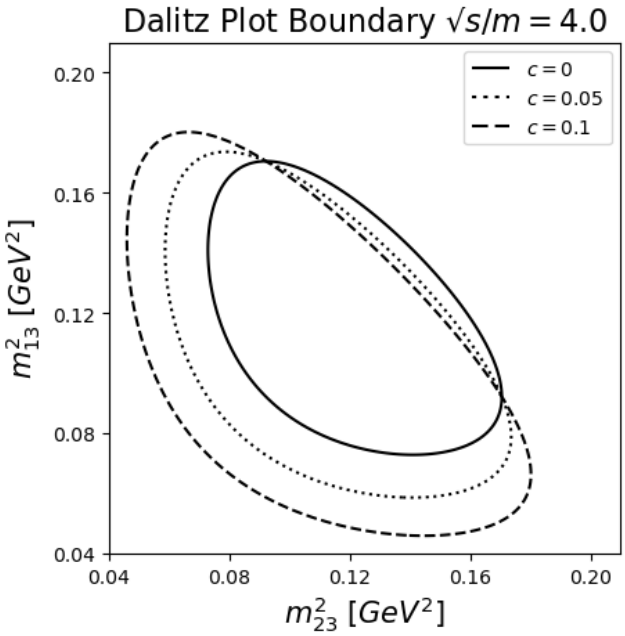

Figure 4.2 Shape of the Dalitz plot for the $\sqrt{s}/m$ value corresponding to $\eta \to 3\pi^0$. The standard outline is shown, along with outlines for two nonzero values of the Lorentz violation parameter c.

decays typically have relativistic outgoing particles, $m^2 \ll |\vec{p}|^2$, $|\vec{k}|^2$, $\sqrt{s}$, we could simplify this expression by dropping those terms that are small in both c and m^2. With this logic, neglecting any term which multiplies both c and m^2, the boundary condition is simplified to

$$\sqrt{s}(1+c) - \sqrt{|\vec{p}|^2 + m^2} - \sqrt{|\vec{k}|^2 + m^2} - c|\vec{p}| \lesseqgtr \sqrt{|\vec{k}|^2 + |\vec{p}|^2 + m^2 \mp 2|\vec{p}||\vec{k}|} \quad (4.28)$$

which is almost as simple as the conventional boundary condition with vanishing c.

The Dalitz plot is affected by the Lorentz violation through the modified boundary condition. The boundary line for this plot can be plotted in terms of the unmod-

ified invariant mass-squared parameters, which are given in terms of the unmodified single-particle energies,

$$p^{(0)} = \sqrt{|\vec{p}|^2 + m^2} = \frac{s + m^2 - m_{13}^2}{2\sqrt{s}} \tag{4.29}$$

$$k^{(0)} = \sqrt{|\vec{k}|^2 + m^2} = \frac{s + m^2 - m_{23}^2}{2\sqrt{s}}, \tag{4.30}$$

which are plugged into the boundary (4.28).

This Dalitz plot boundary line is given by a modified quartic equation in the invariant mass squared parameters m_{13}^2 and m_{23}^2. With a $c = 0$ and all the daughter particle masses the same the boundary equation is

$$0 = (m_{13}^2)^2 m_{23}^2 + m_{13}^2 (m_{23}^2)^2 - (3m^2 + s) m_{13}^2 m_{23}^2 + (m^2 - s)^2 m^2. \tag{4.31}$$

With the inclusion of Lorentz violation term, the exact quartic is extremely intricate, but to leading order in c it takes the tractable form

$$\begin{aligned} 0 = {} & (m_{13}^2)^2 m_{23}^2 + m_{13}^2 (m_{23}^2)^2 - (3m^2 + s) m_{13}^2 m_{23}^2 + (m^2 - s)^2 m^2 \\ & + \frac{c}{2s}((m^2 - s - m_{23}^2 - m_{13}^2)(2m^2 - m_{23}^2 - m_{13}^2) \cdot \\ & \cdot (m^4 - s^2 + m_{23}^2 m_{13}^2 - m^2(m_{23}^2 + m_{13}^2) + s(m_{23}^2 + m_{13}^2))) \end{aligned} \tag{4.32}$$

The boundary line is plotted in the m_{23}^2-m_{13}^2 plane. Setting the quantity c to zero as in (4.31) naturally gives the standard outline of the plot. In this case, the elongation of the curve depends only on the available decay energy compared with the common mass of the daughters, $\sqrt{s}/m$. When c is increased to a nonzero value the boundary plot shifts according to (4.32). This is linked to the fact that under Lorentz transformation, the allowed physical region will be rotated and shifted

relative to a frame with no Lorentz violation. Increasing the c term in the modified plot is associated with enlarging the physically allowed parameter region, as well as generally shifting it towards smaller values of m_{13}^2, m_{23}^2, and (redundantly) m_{23}^2.

Figure 4.2 shows the effect of c on the shape of the Dalitz plot for a decay with $\sqrt{s}/m = 4.0$, very close to the value for 3.97 for the physical decay $\eta \to 3\pi^0$. Increasing the strength of the Lorentz violation (in this specific model), shifts the kinematically allowed region towards smaller values of m_{23}^2 and m_{13}^2—in a symmetric fashion, because the daughter particles are identical. Precision measurements of this particular decay are already recognized to be important, since the matrix element, calculated using chiral perturbation theory, depends directly on the isospin-violating up-down mass difference, $m_d - m_u$ [3, 46, 57]. Measurements of this and similar processes continue to be used for state-of-the-art measurements of this important parameter in low-energy flavor physics [41, 5].

In figures 4.3 and 4.4, we show the analogous shape of the Dalitz plots for hypothetical higher-energy decays. Figure 4.3 shows a moderately more relativistic case, with $\sqrt{s}/m = 6.5$, while figure 4.4 displays a Dalitz plot for a situation in which the daughter pions are in the strongly relativistic regime. As the shape becomes increasingly triangular, we can see that it correspondingly becomes relatively less sensitive to the variety of Lorentz violation that we have considered. This appears to be a generic feature of $c_{\mu\nu}$-type Lorentz violation. This is perhaps not unexpected, with a $c_{\mu\nu}$ coefficient tending to shift the boundaries of kinematically allowed regions by less as the pion masses become less important and the energy-momentum relations for the outgoing particles become more nearly linear.

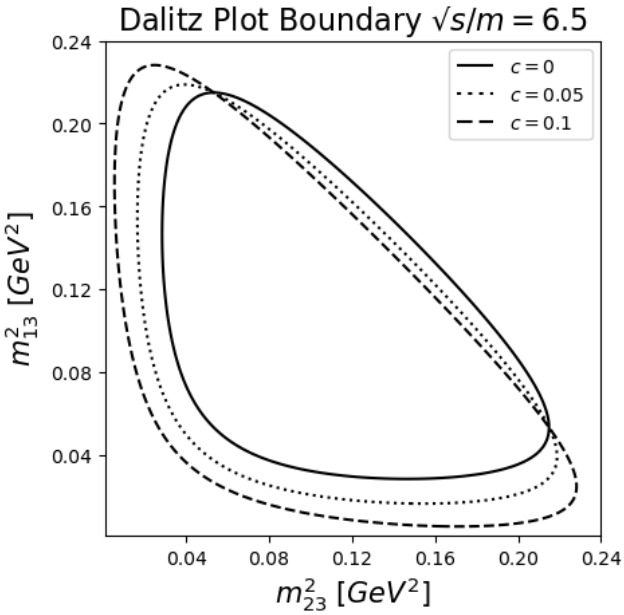

Figure 4.3 Shape of the Dalitz plot for a $\sqrt{s}/m = 6.5$ value.

With time-stamped and pion tracking data, it would also be possible to search these data sets for evidence of Lorentz violation. This would entail constructing separate Dalitz plots for different bins of sidereal time, so see whether the kinematically allowed regions shifts around in the m_{23}^2-m_{13}^2 plane as the laboratory rotates with the Earth. As the laboratory rotates, the structure of the 3×3 matrix of anisotropy coefficients c_{jk} will change. However, to analyze this will necessarily mean consideration of more complicated c_{jk} textures than we have so far considered here; even if the form of Lorentz violation may be described by a single parameter c at one particular moment, at a different sidereal time, the rotation of the laboratory will change the structure of the lab-frame c_{jk} coefficient matrix. There have been some

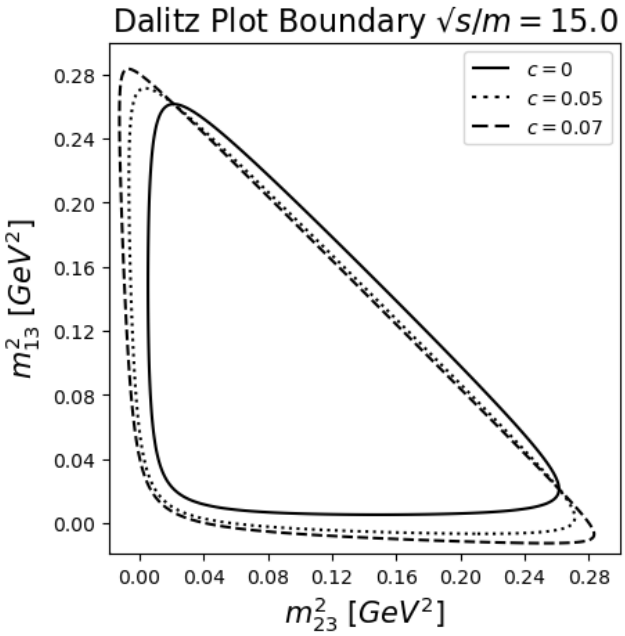

Figure 4.4 Shape of the Dalitz plot for an ultrarelativistic value of $\sqrt{s}/m = 15.0$.

previous consideration of how reaction thresholds for particle processes would change with the Earth's rotation, but the Dalitz plot provides a more general structure. It would be possible, for instance, to look at the m_{23}^2 threshold for a decay—which is represented by the left-most point on the outline of a Dalitz plot—and how this quantity depends on a given type of Lorentz violation. However, the full outline gives significantly more information than just observation of a single threshold.

4.5 Conclusions and Outlook

Dalitz plots are widely used in the analysis of three-body decays (especially decays into spinless particles). The histogram in the interior of the Dalitz plot region is

sensitive to variations (particular resonance thresholds) in the decay matrix element, while the outline of that region is determined by the decay kinematics. We have looked at how this outline is affected by Lorentz violation of the $c_{\mu\nu}$ type, focusing on specific illustrative models with broken boost and rotation symmetries. The Lorentz violation changes the shape of the outline for three-pion decays, with more pronounced fractional changes at lower values of $\sqrt{s}/m$.

Lorentz violation affecting unstable particle species is much harder to bound than similar violations for the constituents of everyday matter. The shapes of Dalitz plots for decays into heavy mesons may be good observables for constraining SME coefficients in those sectors. For realistic studies, it could be useful to construct separate Dalitz plots in bins of sidereal time, so that evidence of changes in the shape as a source beam's direction changes. It would also be natural to consider more general textures for the tensor background $c_{\mu\nu}$.

Analyses of the effects of Lorentz violation on the Dalitz plots for weak decays are more complicated than what we have considered in this paper, for a couple of different reasons. Firstly, the daughter particles in such decays are not identical, so the SME coefficients for multiple sectors of the Standard Model will come into play. Secondly, the decays involve fermions, for which there are additional spin-dependent SME parameters beyond the $c_{\mu\nu}$. Work on understanding the effects of these complexities is ongoing.

Chapter 5

Overall review of Research findings

5.1 Conclusions and Extensions

Everything we know about interactions of particles is based on symmetries of some form. Moreover, the development of relativity contributed tremendously to our understanding of the critical importance of symmetries in physics and has contributed largely to the development of the Standard Model of particle physics. The main problem in physics has to do with the unification of the two major theories to one unified theory of quantum gravity. Therefore, there exist important observations that are left unresolved by the Standard Model which bring the reasoning and motivation to search for exotic physical phenomena. In composing beyond Standard Model extensions for the exact theory of nature, symmetries and symmetry violations serve as a guiding tool.

Discussion of the inclusion of Lorentz and CPT violation for scenarios in radiation emission, scattering cross sections, and decay rates, along with modified versions of Dalitz plots have been explored and modeled in this dissertation research. To summarize the Standard Model and extend it further, we gave the basic concepts and outlined the experimental techniques for search of Lorentz violation signatures.

In chapter 3 we have found that it is interesting to ask how the elaborate details of radiation theory will change in the presence of Lorentz-violating preferred backgrounds like k^{μ}_{AF}. Many useful techniques have been developed for making quantitative calculations of tricky quantities in Maxwellian electrodynamics and for understanding their qualitative characteristics. To what extent these methods continue to be useful—and what adjustments are needed to keep them so—in a theory with exotic modifications to the charged particle and photon sectors may provide insights

both into the specific theories being considered and the general structure of classical (or quantum) radiation processes.

In our classical treatment, we examined one of the standard loci for studying electromagnetic wave emission—the radiation from an oscillating electric dipole—in a model in which the electromagnetic sector is modified to include novel CPT- and Lorentz-violating propagation effects involving a preferred axial vector background. We evaluated the vacuum-birefringent radiation fields, including non-perturbative terms where appropriate. In general, the energy-momentum carried by the fields in this model is known to have a complicated non-perturbative structure, which cannot be captured by naive power series expansions in the components of the preferred background vector. However, we nevertheless find that at the lowest nontrivial orders, there are actually no modifications to the Larmor expressions for the energy-momentum emission.

The natural extension of this case considered in chapter 3 would be to look at higher multipoles, but this would likely not result in higher-order modifications to the total radiation rate. Therefore, it is reasonable to assume that using harmonically oscillating source in electrodynamics to search for Lorentz violating effects is probably not worth further analyzing. However, the theory could be quantized and the radiation studied in that context. Or the methods could be carried over to a model like that of Chern-Simons gravity, in which gravitational radiation from harmonic source might still be modified.

In chapter 4, on our quantum and kinematics considerations in the Standard Model Extension, we found that rates for particle interaction processes and decays

will be modified in a Lorentz-violating quantum field theory because of changes to the particle kinematics—particularly through the modified dispersion relations affecting the outgoing particle phase space. We outlined these changes to the rates for three-particle decays. Considering a process with a constant scattering amplitude (not directly modified by the Lorentz violation), we calculate leading order corrections to the kinematics for a decay into three identical spinless particles whose propagation is affected by a $c_{\mu\nu}$-type symmetric tensor background. We examine the angular distribution of the daughter particles and describe the shape of the corresponding Dalitz plot outlining the kinematically allowed region, according to two toy models for the $c_{\mu\nu}$ textures. Precision measurements of the boundaries of this region could be used to constrain Lorentz violation coefficients for the particles involved in processes such as $\eta \to 3\pi^0$. The result for our decay analysis is that although Dalitz plots of this type can be used to bound coefficients, to get something experimentally observable, the process would need to be evaluated in the presence of a more realistic time-dependent type of Lorentz violation in the lab frame, which would involve a more intricate and complicated analysis. We thus found extensions to real physical theories within the minimal SME framework and how momentum and energy is modified and what implications this has on the dynamics and kinematics of specific particle processes.

Future analyses of three-body decays involving Lorentz violation may focus particularly on muon decays, $\mu^\pm \to e^\pm + \nu + \bar{\nu}$. Muon physics has proved to be a fruitful source for bounds on coefficients in sectors of the SME that are otherwise hard to constrain. In [49], the authors used muon decay as a tool to test the invariance of

the weak interaction under Lorentz transformations. Further motivation for investigating muon properties comes from the phenomenology of the muon anomalous magnetic moment ("$g-2$") [6, 30] and muonic hydrogen [19], where other puzzling deviations from predictions based on the Standard Model presently exist. Especially for the magnetic moment experiment, where the direct observable is the decay rate, a full understanding of the three-body decay is important.

The muon work was part of a more general development of the use of three-body β-decays to explore Lorentz violations in the weak sector [50, 51, 53, 54, 55, 96], with the SME coefficients only appearing in the virtual $W^{\pm}$ propagator, rather than the external particle kinematics. The kinematic effects in weak three-body decays have also been studied [36]; however, most kinematic analyses of Lorentz violation in β-decays have focused on two-body decays, such as $\pi^+ \to \mu^+ + \nu$; or on Cerenkov-like emission of neutrino-antineutrino pairs, as in the normally forbidden process $p^+ \to p^+ + \nu + \bar{\nu}$, for which the kinematics are (because the neutrinos are nearly massless) essentially the same as those for a Cerenkov process.

Overall, our analysis has been proven to be effective. Even though we did not find at leading order a modified Larmor expression or find a fully realistic SME decay rate, deriving our solutions involved developing theoretical techniques and calculating multiple quantities that will help us understand how radiation and decay structures will be modified at higher order.

As a last note, here we mention further possible research that could lead to very useful results in the future by further extending models already developed in the Standard Model and the SME. These types of models include direct extensions of

this like our toy model, for example in heavy quark effective theory, where there already exist works on D-meson decay in the SME. Another extension as already somewhat discussed is the possibility to extend the SME Chern-Simons theory in the gravity sector to a spacetime with a Gödel-type metric, as is done in [20]. Other interesting topics, still closely aligned to the Standard Model and the already-existing structure of the SME are theories with n-Higgs doublet: models which contain a large number of $SU(2)_L$-preserving accidental symmetries as subgroups of the symplectic group $Sp(2n)$. (For example, in cases with 2- and 3-Higgs doublet potentials, 13 and 40 accidental symmetries are found.) [73] Another which already exists in the SME is that of supersymmetric models where theories contain infinite sets of conservation laws [69]. One last example is that of chiral perturbation theory, which is an EFT of quantum chromodynamics for energies below 1 GeV, formulated in terms of color-neutral hadrons, which has been extended [23] to include Lorentz-violating operators formulated out of quarks and gluons; maybe the possibility of obtaining a unique method for evaluating vertices with less than four pions can be further considered.

Bibliography

[1] M. A. Gonzalez Leon A. Alonso Izquierdo W. Garcia Fuertes and J. Mateos Guilarte. Nucl. Phys. B. **635** 525, (2002).

[2] F. Kirk A. Crivellin and M. Schreck. JHEP. **11** 109, (2022)[arXiv:2208.11420].

[3] H. Leutwyler A. V. Anisovich. Phys. Lett. B. **375** 335, (1996).

[4] O. Randriamboarison A.D.A.M. Spallicci G. Sarracino and J.A. Helayel-Neto. [arXiv:2205.02487].

[5] M. Ablikim. et al. (BESIII Collaboration), Phys. Rev. D. **107** 092007, (2023).

[6] D. P. Aguillard. et al. (Muon $g-2$ Collaboration), Phys. Rev. D. **110**, 032009, (2024).

[7] K.K. Vos et al. Phys. Rev. Lett. B. **729** 112, (2014).

[8] S. Herrmann et al. Phys. Rev. Lett. **95** 150401, (2005).

[9] B. Altschul. EPL. **135** 41001, (2021).

[10] B. Altschul. Phys. Rev. D. **70** 101701, (2004).

[11] B. Altschul. Phys. Rev. D. **99** 125009, (2019).

[12] B. Altschul. Phys. Rev. D. **74** 083003, (2006).

[13] B. Altschul. Phys. Rev. D. **75** 105003, (2007).

[14] B. Altschul. Phys. Rev. D. **70** 056005, (2004).

[15] B. Altschul. Phys. Rev. D. **79** 016004, (2009).

[16] B. Altschul. Phys. Rev. Lett. **96** 201101, (2006).

[17] B. Altschul. Phys. Rev. Lett. **98** 041603, (2007).

[18] B. Altschul. Symmetry. **9** 250, (2017).

[19] A. Antognini. et al., Science. **339** 417, (2013).

[20] A. Yu. Petrov (Paraiba U.) B. Altschul J.R. Nascimento (Paraiba U.) and P.J. Porfirio (Paraiba U.) Class. Quant. Grav. **39** 2, 025002, (2021).

[21] D. Colladay B. Altschul. Phys. Rev. D. **71** 205298, (2005).

[22] J. O'Connor B. Altschul. Submitted Phys. Rev. D. **x** arXiv 2506.19564, (2025).

[23] M. Schindler B. Altschul. Phys. Rev. D 100. **7** 075031, (2019).

[24] F. R. Klinkhamer C. Adam. Nucl. Phys. B. **607** 247, (2001).

[25] Ulf-G. Meißer C. Ditsche B. Kubis. Eur. Phys. J. C. **60** 83, (2009).

[26] R. F. Dashen C. G. Callan and D. J. Gross. Phys. Lett. B. **63** 334, (1976).

[27] F. R. Klinkhamer C. Kaufhold. *Nucl. Phys. B.* **734** 1, (2006).

[28] S.M. Carroll and G.B. Field. Phys. Rev. Lett. **79** 2394, (1997)[arXiv:astro-ph/9704263].

[29] J. M. Chung. Phys. Rev. B. **461** 138, (1999).

[30] G. Colangelo. et al. arXiv:2203.15810, (2022).

[31] M. Taiuti D. Anselmi. Phys. Rev. D. **83** 056010, (2011).

[32] V. A. Kostelecký D. Colladay. Phys. Lett. B. **511** 209, (2001).

[33] V. A. Kostelecký D. Colladay. Phys. Rev. D. **55** 6760, (1997).

[34] V. A. Kostelecký D. Colladay. Phys. Rev. D. **58** 116002, (1998).

[35] A. J. Hariton D. Guarrera. Phys. Rev. D. **76** 044011, (2007).

[36] J. S. Díaz. Adv. High Energy Phys. **2014** 205298, (2014).

[37] Q. Exirifard. Phys. Rev. B. **699** 1, (2011).

[38] M. Risse F. Duenkel M. Niechciol. Phys. Rev. D. **104** 015010, (2021).

[39] C. Rupp F. R. Klinkhamer. Phys. Rev. D. **70** 045020, (2001).

[40] S. Majid G. Amelino-Camelia. Int. J. Mod. Phys. A. **15** 431, (2000).

[41] H. Leutwyler G. Colangelo S. Lanz and E. Passemar. Phys. Rev. Lett. **118** 022001, (2017).

[42] O. W. Greenberg. Phys. Lett. B. **89** 231602, (2002).

[43] S. Hossenfelder. Adv. High Energy Phys. **2014** 950672, (2014).

[44] R. Roiban I. Mocioiu M. Pospelov. Phys. Lett. B. **489** 390, (2000).

[45] L. F. Urrutia J. Alfaro H. A. Morales-Técotl. Phys. Rev. D. **65** 103509, (2002).

[46] K. Ghorbani J. Bijnens. JHEP. **11** 030, (2007).

[47] A. Salam J. Golstone and S. Weinberg. Phys. Rev. Lett. **3** 127, (1962).

[48] B. Altschul J. O'Connor. Phys. Rev. D. **109** 045005, (2024).

[49] H. W. Wilschut J. P. Noodmans C. J. G. Onderwater and R. G. E. Timmermans. Phys. Rev. D. **93**, (2016).

[50] R. G. E. Timmermans J. P. Noordmans H. W. Wilschut. Phys. Rev. C. **87** 055502, (2013).

[51] R. G. E. Timmermans J. P. Noordmans H. W. Wilschut. Phys. Rev. Lett. **111** 171601, (2013).

[52] F. R. Klinkhamer K. J. B. Ghosh. Nucl. Phys. B. **926** 335, (2018).

[53] R. G. E. Timmermans K. K. Vos H. W. Wilschut. Phys. Rev. C. **91** 038501, (2015).

[54] R. G. E. Timmermans K. K. Vos H. W. Wilschut. Phys. Rev. C. **92** 205298, (2015).

[55] R. G. E. Timmermans K. K. Vos H. W. Wilschut. Rev. Mod. Phys. **87** 1483, (2015).

[56] B. Altschul K. Schober. Phys. Rev. D. **92** 125016, (2015).

[57] Marc Knecht Karol Kampf. Phys. Rev. D. **84** 114015, (2011).

[58] F. R. Klinkhamer. Nucl. Phys. B. **535** 233, (1998).

[59] F. R. Klinkhamer. Nucl. Phys. B. **578** 277, (2000).

[60] V. A. Kostelecký. Phys. Rev. D. **69** 105009, (2004).

[61] V. A. Kostelecký and C.D. Lane. Phys. Rev. D. **60** 116010, (1999).

[62] M. Lembo L. Caloni S. Giardiello et al. JCAP. **03** 018, (2023).

[63] M. Lembo L. Caloni S. Giardiello et al. JCAP. **03** 018, (2023)[arXiv:2212.04867].

[64] H.A. Furst L.S. Dreissen C.H. Yeh, K.C. Grensemann, and T.E. Mehlstaubler. Nature Commun. **13** 7314, (2022)[arXiv:2206.00570].

[65] C.D. Lane. Phys. Rev. Lett. **91** 190403, (2003).

[66] G. B. Field M. A. Berger. J. Fluid Mech. **147** 133, (1984).

[67] H. Sahlmann M. Bojowald H. A. Morales-Técotl. Phys. Rev. D. **71** 084012, (2005).

[68] J. A. A. S. Reis M. Shreck. Phys. Rev. D. **103** 095029, (2021).

[69] V. A. Kostelecký M.S. Berger. Phys. Rev. D. **65** 091701, (2001).

[70] M. Mewes. Phys. Rev. D. **78** 096008, (2008).

[71] M. Mewes. Phys. Rev. D. **78** 096008, (2008)[arXiv:1604.01102].

[72] H. K. Moffat. J. Fluid Mech. **35** 117, (1969).

[73] A. Pilaftsis N. Darvishi. Phys. Rev. D. **101** 9, 095008, (2020).

[74] M. M. Ferreira P. D. S. Silva L. Lisboa-Santos and M. Schreck. Phys. Rev. D. **104** 116023, (2021).

[75] M. Pérez-Victoria. JHEP. **04** 032, (2001).

[76] V. A. Kostelecký R. Bluhm and C.D. Lane. Phys. Rev. Lett. **84** 1098, (2000).

[77] V. A. Kostelecký R. Bluhm and C.D. Lane. Phys. Rev. Lett. **84** 1381, (2000).

[78] V. A. Kostelecký R. Bluhm and N. Russell. Phys. Rev. Lett. **79** 1432, (1997).

[79] V. A. Kostelecký R. Bluhm and N. Russell. Phys. Rev. Lett. **82** 2254, (1999).

[80] B. Altschul R. DeCosta. Phys. Rev. D. **97** 055029, (2018).

[81] J. Pullin R. Gambini. Phys. Rev. D. **59** 124021, (1999).

[82] F. Kislat R. Gerasimov P. Bhoj. Symmetry. **13** 880, (2021).

[83] S.-Y. Pi R. Jackiw. Phys. Rev. D. **68** 104012, (2003).

[84] V. A. Kostelecký R. Jackiw. Phys. Rev. Lett. **82** 3572, (1999).

[85] R. Potting R. Lehnert. Phys. Rev. D. **70** 125010, (2004).

[86] N. Yunes S. Alexander. Phys. Rev. Lett. **99** 241101, (2007).

[87] F. R. Klinkhamer S. Bernadotte. Phys. Rev. D. **75** 024028, (2007).

[88] S. L. Glashow S. Coleman. Phys. Rev. D. **59** 116008, (2014).

[89] B. Altschul S. Karki. Phys. Rev. D. **102** 035009, (2020).

[90] G. B. Field S. M. Carroll. Phys. Rev. Lett. **79** 2394, (1997).

[91] R. Jackiw S. M. Carroll G. B. Field. Phys. Rev. D. **41** 1231, (1990).

[92] V. A. Kostelecký S. M. Carroll J. A. Harvey, C. D. Lane, and T. Okamoto. Phys. Rev. Lett. **87** 141601, (2001).

[93] M. Schreck. Phys. Rev D. **96** 095026, (2017).

[94] J. S. Schwinger. Phys. Rev. **125** 397, (1962).

[95] F.W. Stecker and S.L. Glashow. Astropart. Phys. **16** 97, (2001).

[96] A. Sytema. et al., Phys. Rev. C. **94** 025503, (2016).

[97] S. Liberati T. Jacobson and D. Mattingly. Nature (London). **424** 1019, (2003).

[98] A. G. M. Pickering V. A. Kostelecký C. D. Lane. Phys. Rev. D. **65** 056006, (2002).

[99] M. J. Perry V. A. Kostelecký R. Lehnert. Phys. Rev. D. **68** 123511, (2003).

[100] M. Mewes V. A. Kostelecký. Phys. Rev. Lett. **87** 251304, (2001).

[101] M. Mewes V. A. Kostelecký. Phys. Rev. Lett. **99** 011601, (2007).

[102] M. Mewes V. A. Kostelecký. Phys. Rev. Lett. **110** 201601, (2013).

[103] M. Mewes V. A. Kostelecký. Phys. Rev. Lett. **97** 140401, (2006).

[104] M. Mewes V. A. Kostelecký A. C. Melissinos. Phys. Lett. B. **761** ,1, (2016).

[105] N. Russell V. A. Kostelecký. Rev. Mod. Phys. **83** 11, (2011).

[106] R. Potting V. A. Kostelecký. Nucl. Phys. B. **359** 545, (1991).

[107] S. Samuel V. A. Kostelecký. Phys. Rev. D. **39** 683, (1989).

[108] N. Ohmae Y. Michimura N. Matsumoto et al. Phys. Rev. Lett. **110** 200401, (2013).